Kansas Geological Survey

Approximate Analysis of Aquifer Mineralization by Paleodrainage Channels

By

Hillel Rubin* and Robert W. Buddemeier
Kansas Geological Survey, The University of Kansas
Lawrence, KS 66047

Kansas Geological Survey Open File Report 98-42
September 27, 1998

GEOHYDROLOGY

The University of Kansas, Lawrence, KS 66047 Tel. (785) 864-3965

Approximate Analysis of Aquifer Mineralization by Paleodrainage Channels

by

Hillel Rubin[1] and Robert W. Buddemeier
Kansas Geological survey, The University of Kansas,
Lawrence, Kansas 66047, USA

ABSTRACT

Mineralization of groundwater resources in south central Kansas can occur due to the penetration of saline water from deep bedrock formation, into small bedrock features of high permeability located in places occupied by streams and rivers in past geological eras. These geological formations are termed "paleodrainage channels." The comparatively fast migration of saline water through these channels of high permeability is associated with the transfer of salinity into the overlying freshwater aquifer. The permeability of the overlying aquifer is significantly smaller than that of the "channel formation". This study develops a set of boundary layer (BL) approaches to quantify the process of salinity transfer from the channels into the aquifer. The methods used in the present study provide quick estimation and evaluation of the dilution of the channel flow, as well as of the salinity profile changes in the mineralized zone created in the overlying aquifer.

The application of the method is exemplified by a complete set of calculations characterizing the possible mineralization process at a specific channel in south central Kansas. Sensitivity analyses are performed and provide information about the importance of the various parameters that affect the mineralization process. Some possible scenarios for the aquifer mineralization phenomena are described and evaluated. It is shown that the channel mineralization may create either several stream tubes of the aquifer with high salinity, or many stream tubes mineralized to a lesser extent. Characteristics of these two patterns of aquifer mineralization are quantified and discussed.

[1] On leave from Department of Civil Engineering, Technion - Israel Institute of Technology, Haifa 32000, ISRAEL

INTRODUCTION

This paper contributes to the understanding of major mechanisms and phenomena involved in the mineralization of groundwater in south central Kansas. The region of major phenomena of groundwater mineralization is shown in Fig. 1. The aquifer subject to mineralization is the Great Bend Prairie alluvial aquifer, which overlies bedrock of Cretaceous and Permian age. Various publications provide information concerning the geology of the region (e.g. Latta, 1950; Layton and Berry, 1973; Fader and Stullken, 1978; Cobb, 1980). During the last few years, significant efforts have been invested in measuring salinity distribution in the region (Young, 1992; Whittemore, 1993; Buddemeier et al., 1992; 1994; Young and Rubin, 1998). These measurements are analyzed and used for the identification of sources of salinity (Whittemore, 1993), as well as mechanisms involved in the mineralization processes (Buddemeier et al., 1994). In the framework of these efforts the authors (Rubin and Buddemeier, 1996; 1998a, b, c, d, e) have developed some conceptual and modeling approaches which provide quantitative estimates of phenomena and mechanisms leading to mineralization of the Great Bend Prairie aquifer. Generally, it seems that salinity penetration into the freshwater aquifer occurs in some locations due to direct contact between the fresh and saline water, and in others due to infiltration of saline water from the deep formation through semi-permeable strata into the freshwater aquifer. In most places, clay and shale layers effectively separate the freshwater aquifer from the saline water of the deep formations. Salinity penetrations are probably local phenomena. However, once it penetrates into the freshwater aquifer, the salinity is advected, disperses and thereby contaminates the freshwater resources of the region.

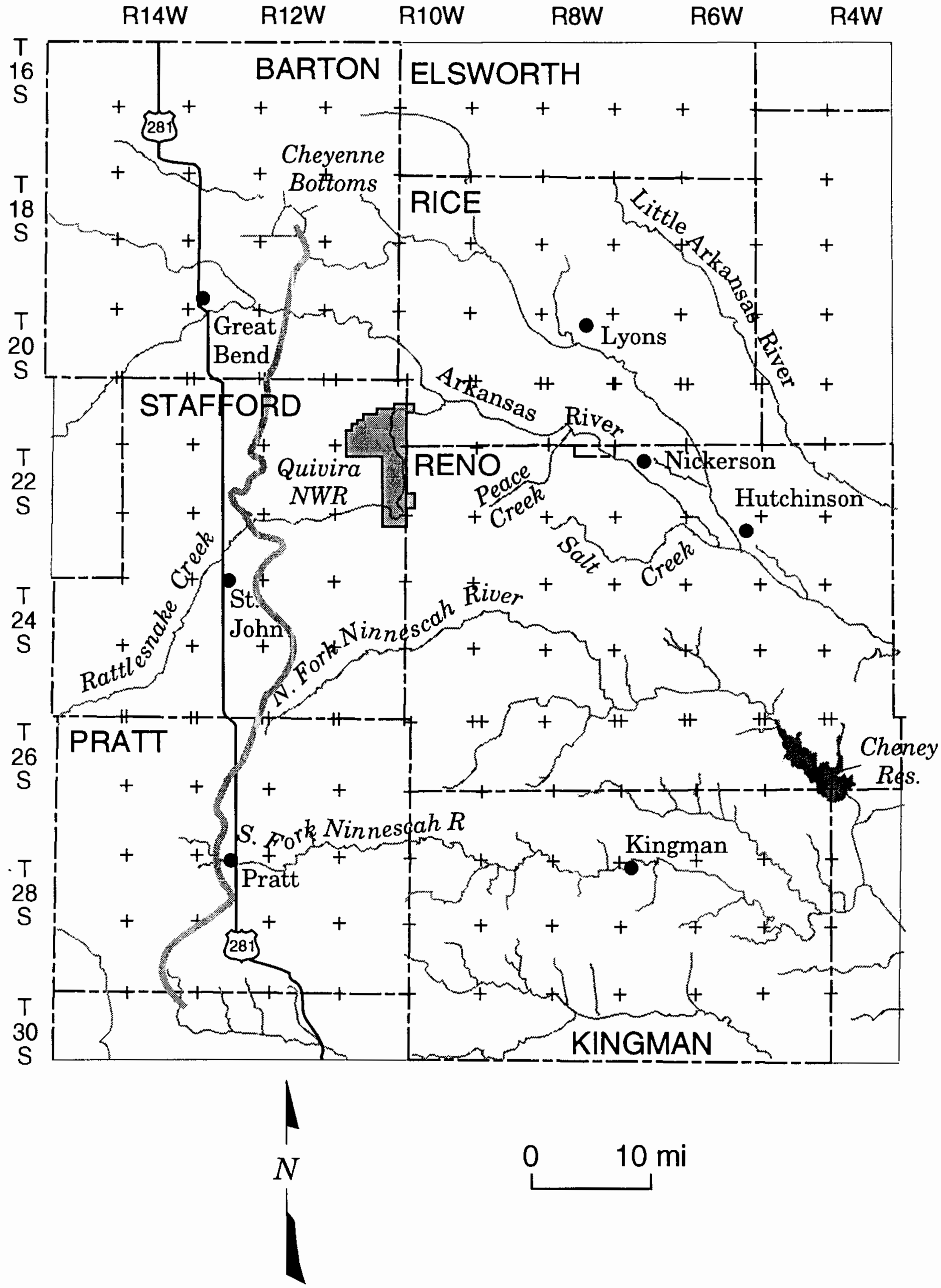

Fig. 1 The region of major groundwater mineralization in south central Kansas. The irregular N-S line near Hwy 281 is the eastern limit of the Cretaceous confining layer (Fig. 2); east of it, groundwater salinity is a problem.

Rubin and Buddemeier (1996) suggested to apply a boundary layer (BL) approach called Top Specified Boundary Layer (TSBL) to analyze a variety of contaminant hydrology issues and problems that could not be analyzed by the traditional BL approaches. The major idea of the TSBL approach is to separate the definition of the region of similar normalized contaminant concentration profiles from the definition of the Region of Interest (ROI), in which contaminant concentration exceeds its acceptable value. Previous studies (Rubin and Buddemeier (1998a, b, c, d), as well as the present one apply the TSBL approach to calculate and evaluate mineralization processes in an inland aquifer.

Sophocleous (1991) reported that in the Great Bend Prairie aquifer a number of highly transmissive bedrock topographic features, termed "paleodrainage channels", exist at the aquifer-bedrock interface. Most of these "channels" emanate from the present day course of the Arkansas River in the area. Sophocleous (1991) provided a review of studies concerning the geology of the region leading to changes in the course of the Arkansas River, and inferred that there are several predominately west-east paleodrainage channels of high permeability in the region, as shown in Fig. 2. By following changes of water level in a grid of monitoring wells Sophocleous (1991) obtained substantial support for the hypothesized existence and effects of paleodrainage channels in the region. Some of these channels are supplied with saline water that discharges from the deep Permian bedrock. The saline water, which enters the channel, may flow along the channel course with a velocity an order of magnitude or more higher than that of the groundwater flowing through the overlying aquifer. The channel water of comparatively high salinity and flow velocity transfers salt into the overlying aquifer groundwater, due to the direct contact between the two types of groundwater. Thus the channel may also act as a secondary source of bedrock salinity by transferring salt into the aquifer at locations distant from the primary discharge out of the bedrock.

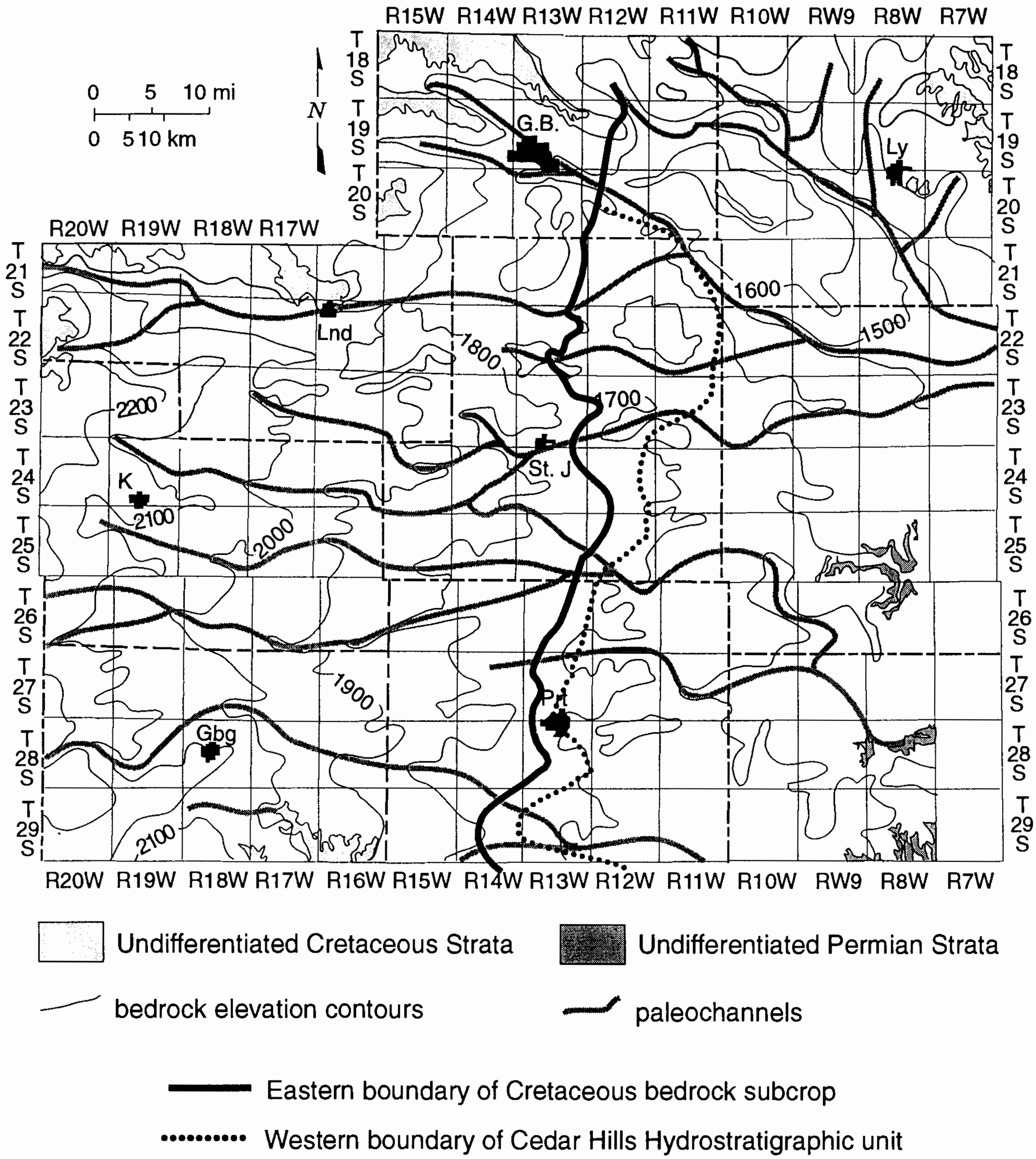

Fig. 2 Pre-Cenozoic bedrock map of the Great Bend Prairie of Kansas with inferred paleodrainage channels. County seats are shown with abbreviated names (Sophocleous, 1991). Substantial saltwater intrusion occurs to the east of the Cretaceous bedrock subcrop.

The present study provides a simplified quantitative analysis of salinity transport in the channels and the overlying aquifer, and suggests a possible set of mechanisms involved in the aquifer mineralization process.

BASIC CONCEPTUAL APPROACH

Figure 3 represents a schematic description of a cross section perpendicular to the channel centerline. It provides some information about sizes and properties of the channel and overlying aquifer assumed for this analysis. The orientation of the channel centerline is commonly different from the direction of the flowlines in the overlying aquifer, and the orientation angle θ between the aquifer flowlines and the channel centerline varies along the channel. As indicated by Fig. 4, the present study refers to two types of channels:

- Curved channel, which crosses a particular flowline once; and
- Winding channel, which crosses some flowlines more than once.

Figure 5 shows the scheme for analyzing salt and water fluxes in an elementary volume of the channel. Owing to the higher salinity of the channel water, diffusion and transverse dispersion transfer salt from the channel into the overlying aquifer. Due to the small width of the channel and the assumed high permeability of its contents, we ignore the channel flow component perpendicular to the channel centerline.

Generally, our calculation of salinity transport through the channel and the overlying aquifer is performed along flowlines of the overlying aquifer.

We consider that the channel flow is completely mixed and salinity distribution in the channel is uniform. Salinity transfer in the overlying aquifer is affected by the build-up of the vertical salinity profile. Effects of dispersion along the flowlines of the aquifer and in the horizontal transverse direction are negligible.

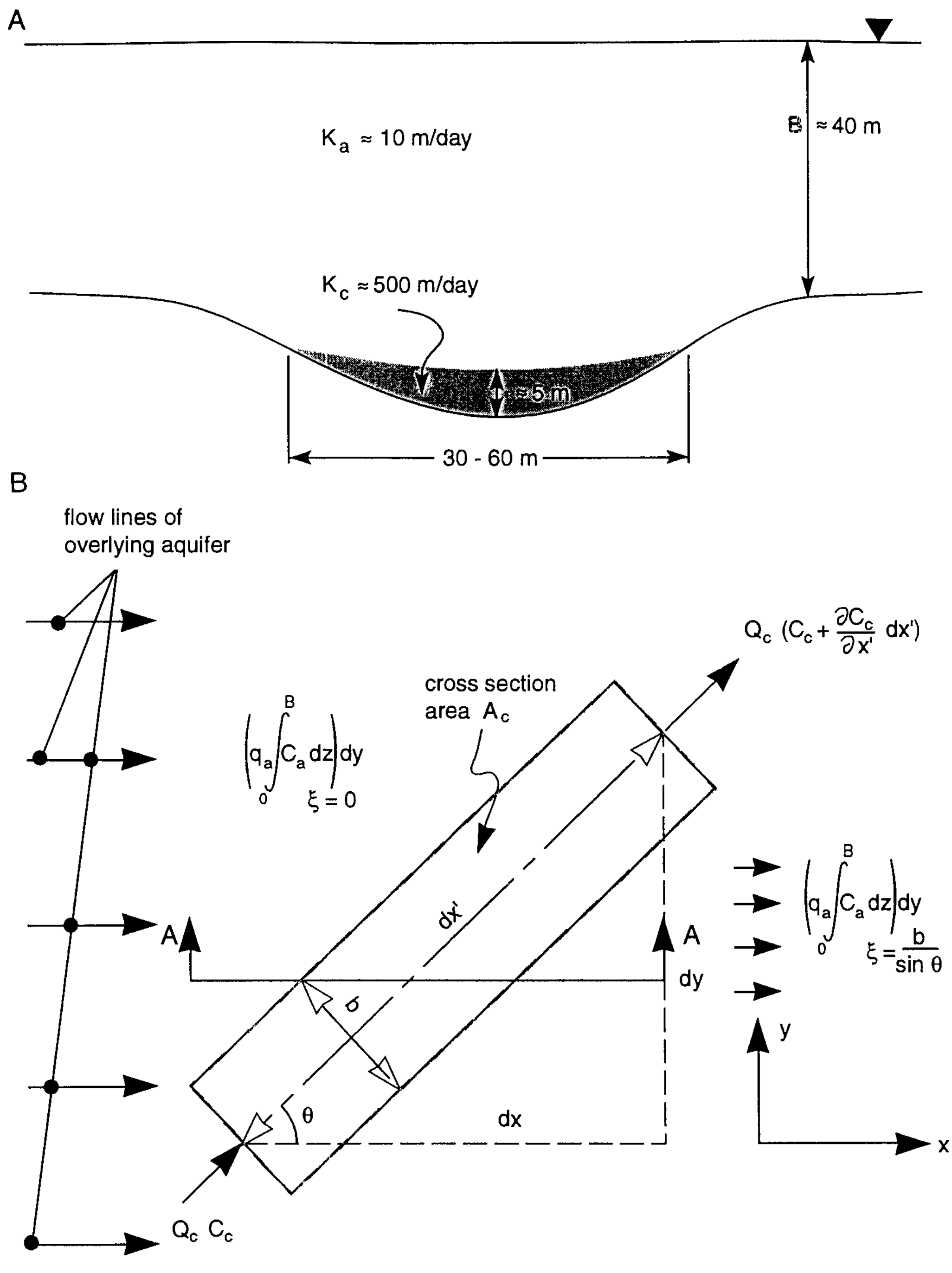

Fig. 3 Cross-section of the aquifer and the paleodrainage channels, illustrating the sizes and hydraulic conductivities used in this study.

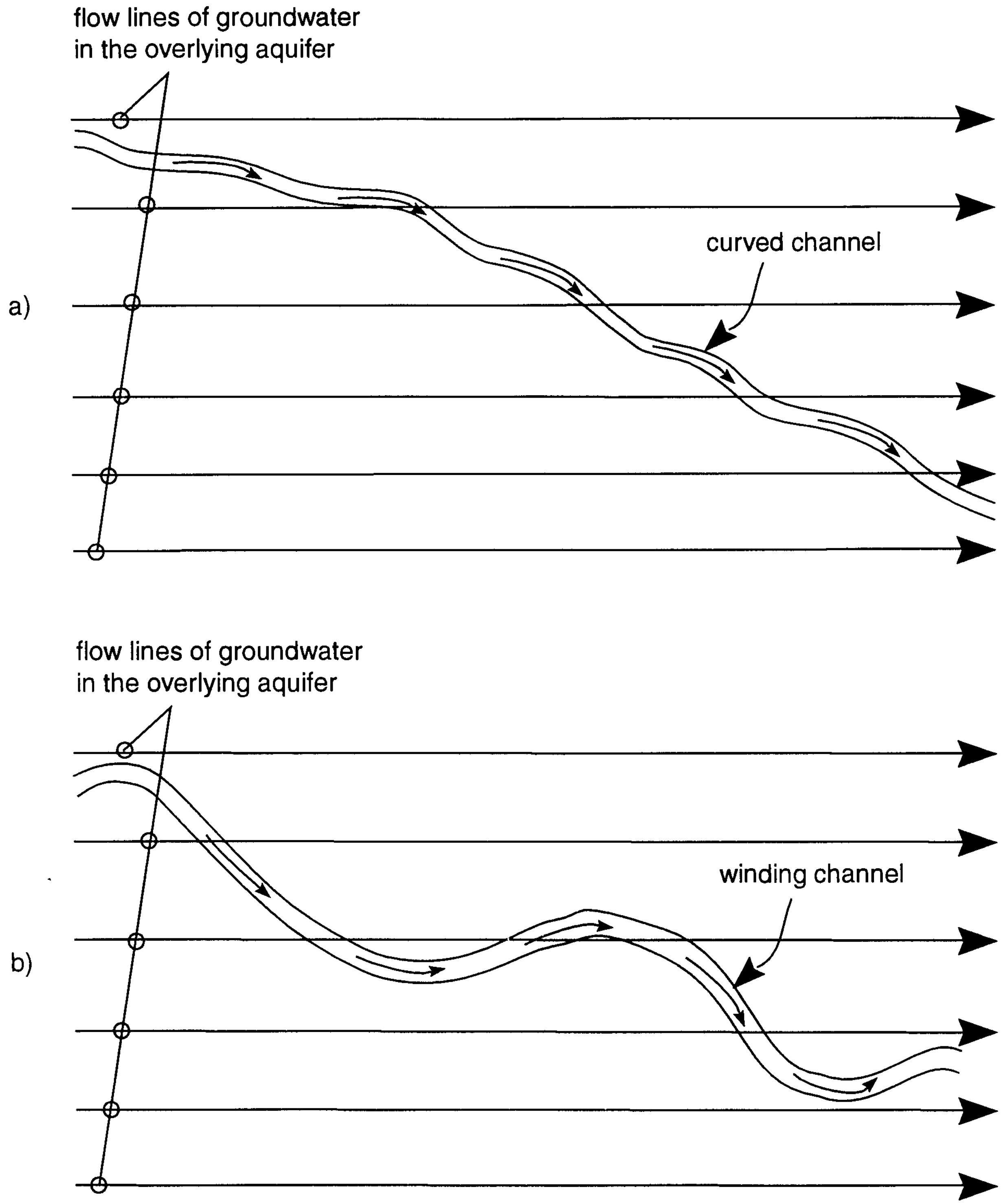

Fig. 4 Types of channels considered in the present study, and their relationship to the aquifer flow.

(a) Curved channel

(b)Winding channel

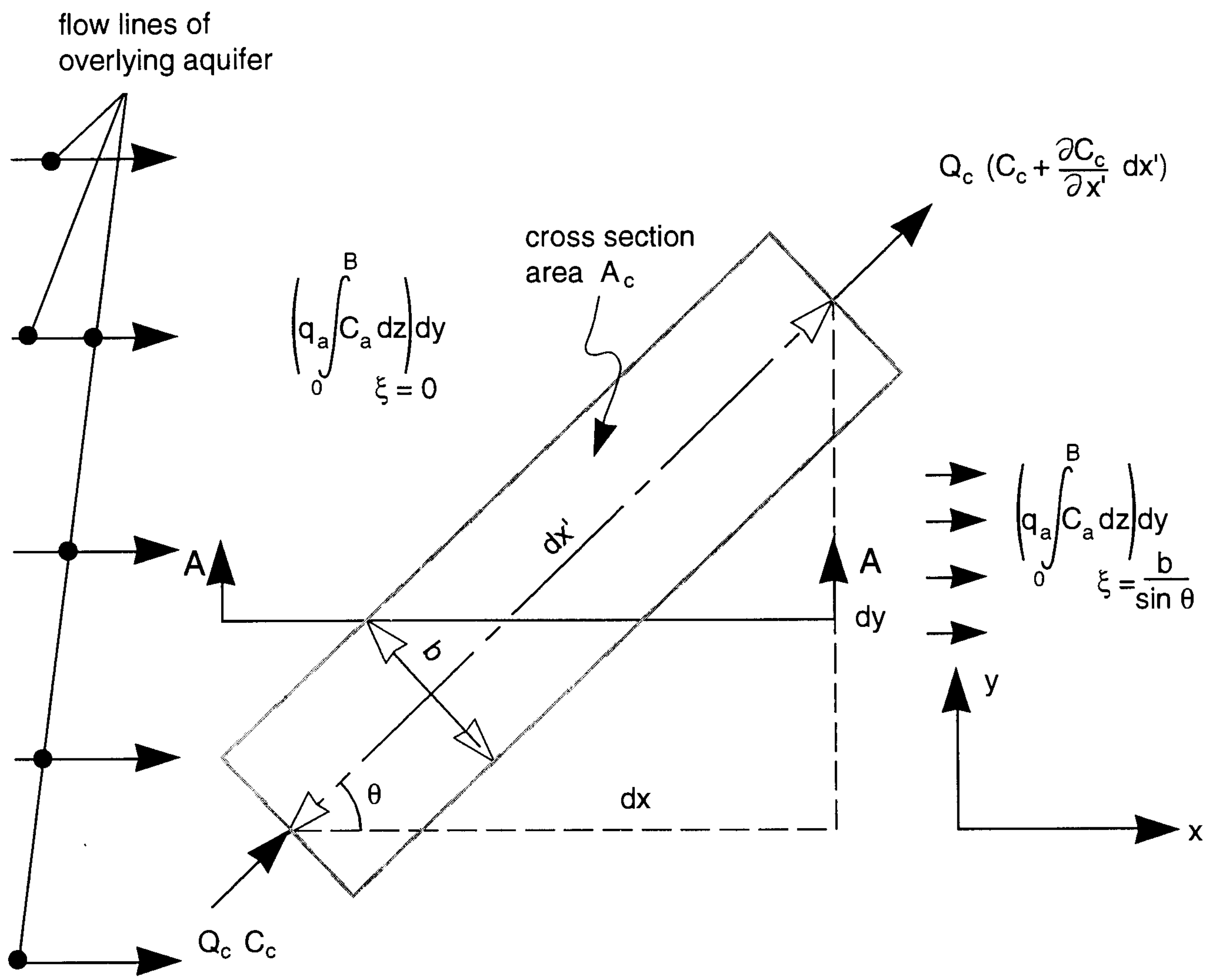

Fig. 5 An elementary volume of the channel with fluxes of channel water, groundwater, and salinity

We consider that due to the comparatively small width of the channel, the salinity profile obtains its steady state shape very quickly along the interface of direct contact between the saline channel water and the overlying aquifer groundwater.

According to Fig. 5, we obtain:

$$A_c\phi_c \frac{\partial C_c}{\partial t}dx' + Q_c \frac{\partial C_c}{\partial x'}dx' = -q_a\left[\left(\int_0^B C_a dz\right)_{\xi=b/\sin\theta} - \left(\int_0^B C_a dz\right)_{\xi=0}\right]dy \qquad (1)$$

where A_c is the cross section area of the channel; C_c is the salinity (salt concentration) of the channel flow; t is the time; Q_c is the channel flow-rate; C_a is the salinity of the aquifer at a point with vertical distance z above the direct contact interface; z is the vertical coordinate; q_a is the specific discharge of the aquifer flow; x' is a local coordinate extended along the channel centerline; ϕ_c is the porosity of the channel material; B is the aquifer thickness; b is the width of the channel; θ is the angle of orientation of the channel, with regard to the flowlines of the aquifer flow; ξ is a local coordinate originating at the upstream (with regard to the aquifer flowline) edge of the channel extending along the interface of direct contact, and parallel to the x direction; the coordinate x represents the direction of the aquifer flowlines; y is the horizontal coordinate perpendicular to the flowlines. We assume that the channel flow-rate is not significantly affected by minor changes of the channel orientation along its course. Therefore, there are probably some changes in the effective cross section of the channel along its course.

By applying a dimensional analysis calculation, we find that the first term of eq. (1) can be neglected, provided that the component of the channel flow velocity in the direction of the aquifer flowline is much larger than the aquifer flow velocity, namely:

$$V_R = \frac{V_a}{V_c \cos\theta} << 1 \qquad (2)$$

where V_a is the flow velocity in the aquifer; V_c is the channel flow velocity, and V_R is termed "the velocity ratio".

According to Fig. 5, there are the following relationships between the different coordinates:

$$dx' = dx / \cos\theta; \quad dy = dx \tan\theta \tag{3}$$

Introducing the relationships of eqs. (2) and (3) into eq. (1), we obtain:

$$\frac{\partial C_c}{\partial x'} = -\frac{q_a \sin\theta}{Q_c}\left[\left(\int_0^B C_a dz\right)_{\xi=b/\sin\theta} - \left(\int_0^B C_a dz\right)_{\xi=0}\right] \tag{4}$$

As mentioned in preceding paragraphs, we identify two types of channels: (1) curved channels, and (2) winding channels. Besides the graphical description of Fig. 4, we may define curved channels as channels, which transfer salinity only to approaching fresh groundwater of the aquifer. Winding channels transfer salinity to approaching fresh, as well as mineralized groundwater of the overlying aquifer. Winding channels are characterized by multiple direct contact interfaces with some flowlines in the overlying aquifer.

Figure 6 shows some schematics of salinity profile development along the interface of direct contact between the channel and the overlying aquifer. Case (a) refers to a curved channel and the portion of the winding channel subject to initial contact with approaching fresh groundwater of the aquifer. Cases (b) and (c) represent possible salinity profiles of the mineralized aquifer groundwater, which interacts with the channel at the interface of direct contact.

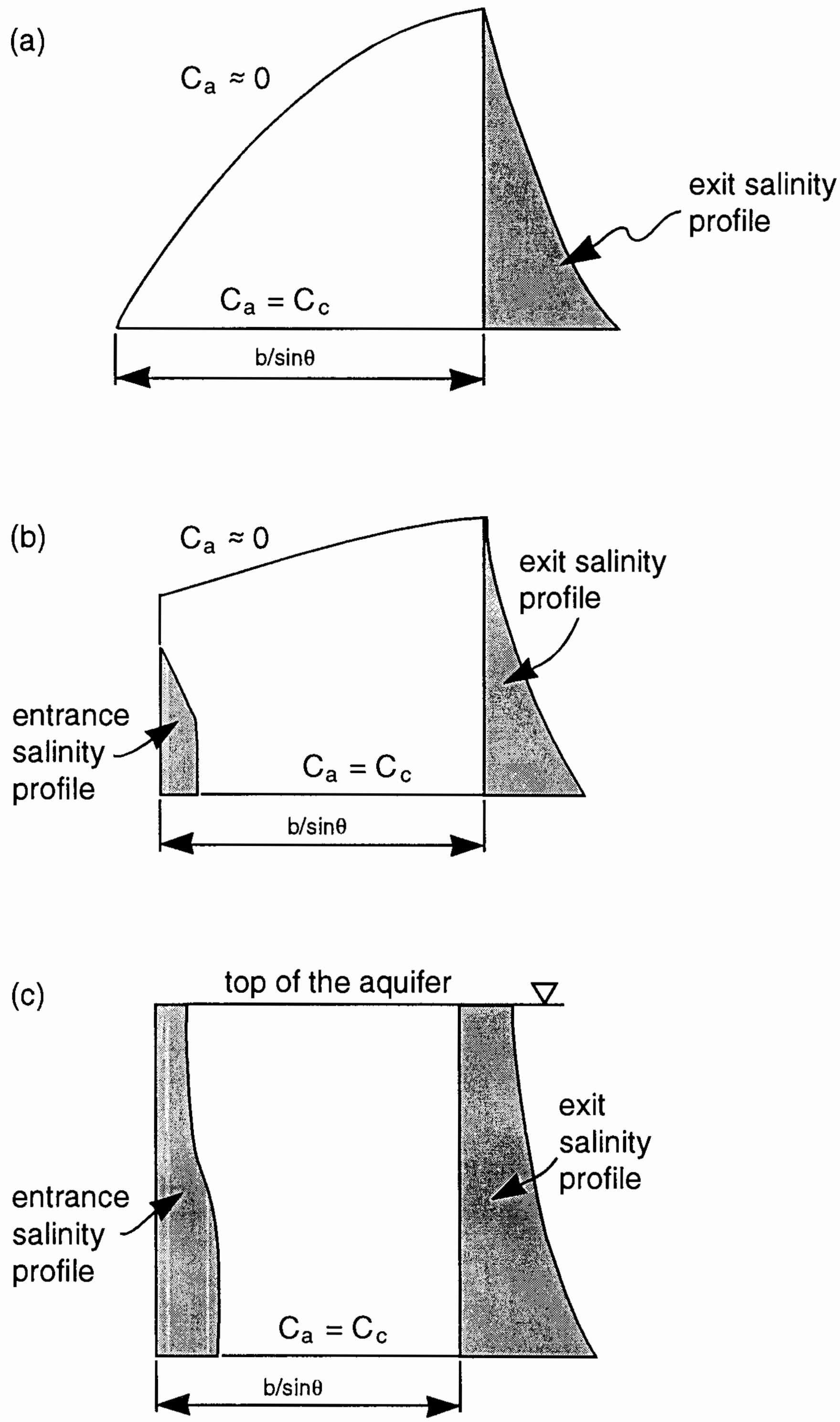

Fig. 6 Build-up of the salinity profile over the direct contact interface

(a) Approaching aquifer groundwater is fresh

(b) (c) Approaching groundwater is mineralized

The interface of direct contact is basically a salinity line source of variable strength. By integrating the salinity flux over the interface it is possible to obtain the total salinity supplied from the channel into the overlying aquifer. Then it is possible to approximate the direct contact interface as a point source and use the image method (e.g., Fischer et al, 1979), to simulate the bottom and top of the aquifer, and thereby obtain an estimate of salinity advection and diffusion in the aquifer. However this approach requires complete uniformity of the domain. Also, use of some of the available semi-analytical solutions of heat conduction in solids (Carslaw and Jaeger, 1959) suffers from similar difficulties. Therefore, in the framework of the present study, it was found appropriate to develop a boundary layer (BL) approach for the analysis and calculation of salinity transport in the aquifer overlying the paleodrainage channels.

The following sections are devoted to the presentation of particular formulations characterizing and quantifying salinity transfer and build-up of salinity profiles in cases of curved and winding channels.

CURVED CHANNELS

In curved channels, the groundwater approaching the channel is always freshwater, since at the upstream edge of the channel, which is represented by $\xi=0$, the aquifer flowline does not carry any salinity. The curved channel calculations are also relevant to the portion of the winding channel which is crossed first by freshwater flowlines of the overlying aquifer. Such flowlines carry freshwater towards the interface of direct contact. Therefore, for such a channel, the second integral of the right-hand side of eq. (1) vanishes. Along the aquifer flowlines, we identify several sections of development of the salinity profile. To enable clear identification of these regions, we define special subsections for each particular flowline. Figure 7 shows the various regions of BL development along the flowline, with the symbols and terminology used in the development that follows (see Notation section for definition of symbols).

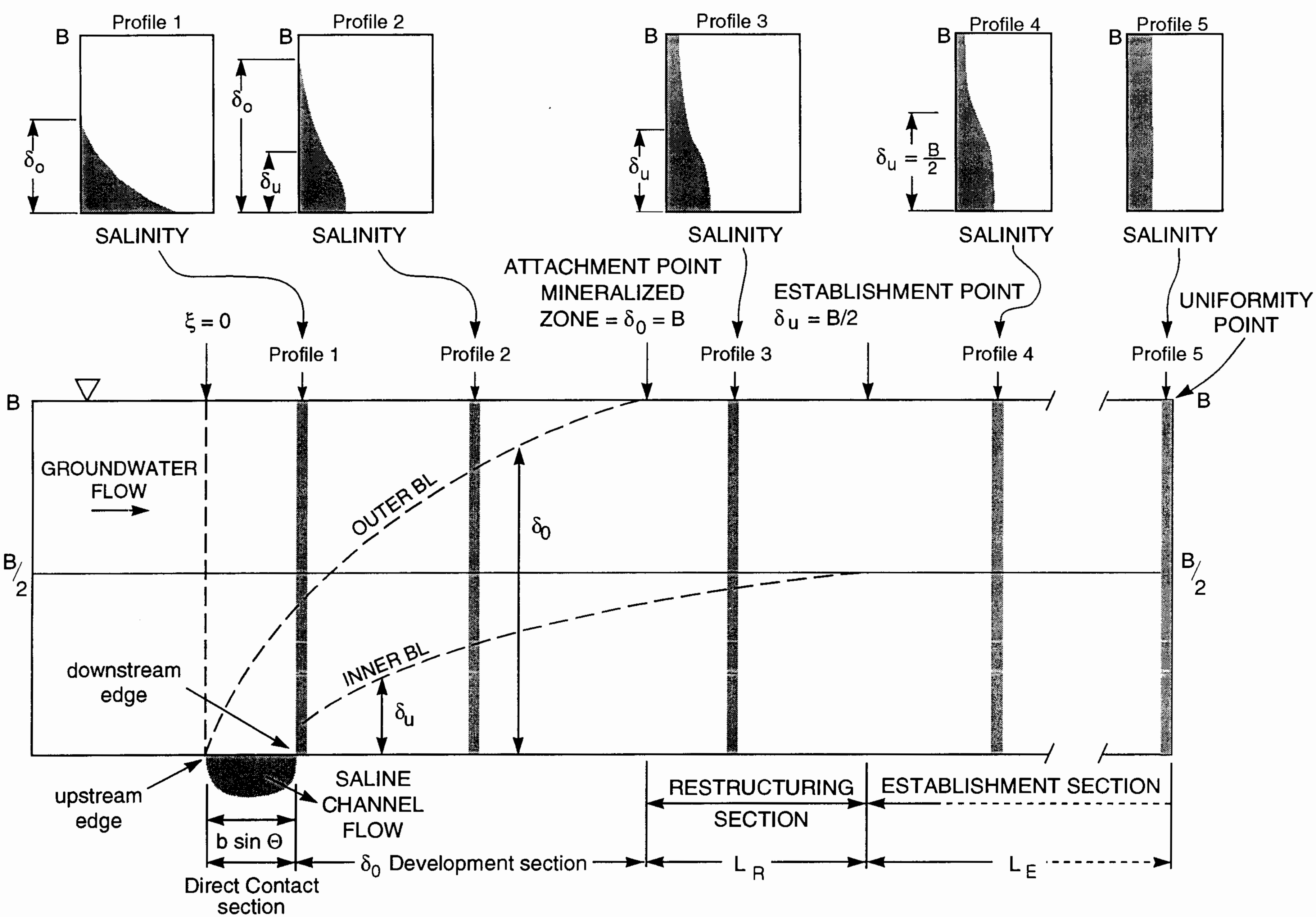

Fig. 7 Characteristics of the various sections of the mineralized aquifer described in this study, with terminology and symbols shown.

The direct contact section

This section is characterized by the interface of direct contact between the channel and overlying aquifer flowlines. We analyze the mineralization process by applying the conceptual approach of the TSBL method (Rubin and Buddemeier, 1966). Owing to the salinity transfer from the channel into the overlying aquifer along the interface of direct contact, there is a build-up of a salinity profile similar to a boundary layer (BL) in the overlying aquifer. Figure 6(a) depicts the development of the BL over the cross section of the channel, which is parallel to the aquifer flowlines. We consider that δ_0 is the thickness of the mineralized portion of the aquifer, which is similar to a BL. The salinity, practically, vanishes at the top of the BL. The salinity is smaller than the acceptable value, C_T, at the top of the region of interest (ROI). The thickness of the ROI is δ, and it is also termed a top specified BL (TSBL). The ROI comprises a portion of the mineralized zone.

According to the BL approximation, the salinity distribution in the overlying aquifer, above the interface of direct contact with the channel, is given by:

$$C_a = C_c\left(1-\frac{z}{\delta_0}\right)^n \tag{5}$$

where δ_0 is the thickness of the mineralized zone, which is a BL; n is a power coefficient approximately equal to 3 (Rubin and Buddemeier, 1996, 1998a).

Due to the small value of the channel width, b, we consider the build-up of the mineralized zone under steady state conditions of flow and salinity distribution. By introducing eq. (5) into the equation of advection-dispersion (Rubin and Buddemeier, 1998a), we obtain the following expression for the build-up of the BL along the interface of direct contact:

$$\left(\delta_0^2\right)_\xi = 2an(n+1)\xi \tag{6}$$

where a is the transverse dispersivity of the aquifer.

By introducing eq. (5) into eq. (4) and integrating over a finite interval $\Delta x'$ along the channel centerline, we obtain:

$$C_c = C_{c0} \exp\left\{ -\int_0^{\Delta x'} \frac{q_a \sin\theta}{Q_c} \left(\delta_0 \int_0^1 (1-\eta)^n d\eta \right)_{\xi = b/\sin\theta} dx' \right\} \tag{7}$$

where C_{c0} is the salinity at a point of reference; η is the BL coordinate, which is given by:

$$\eta = \frac{z}{\delta_0} \tag{8}$$

We introduce eq.(6) into eq. (7) to obtain:

$$C_c = C_{c0} \exp\left\{ -\frac{q_a \Delta x'}{Q_c} \sqrt{\frac{2anb\sin\theta}{n+1}} \right\} \tag{9}$$

Equation (9) can be applied to calculate the variation of C_c along a channel segment, in which values of b, and θ are kept constant. It should be noted that eq. (9) can be applied provided that eq. (2) is satisfied and flow direction in the overlying aquifer is significantly different from the channel centerline direction. Therefore, eq. (9) is not applicable to cases like $\theta = 0, \pi/2$.

Equation (9) indicates that the processes of salinity transfer from the channel into the overlying aquifer occurs along a limited length of the channel and the aquifer. We may consider that if the channel salinity is equal to 1% of its value at the channel entrance then complete dilution of the channel is obtained. Under the condition of complete dilution, practically, the transfer of salinity from the channel flow into the overlying aquifer stops. If a curved channel had constant values of b, and θ, the length of complete dilution of that channel, L_D would be given by:

$$L_D = \frac{4.6 Q_c}{q_a} \sqrt{\frac{n+1}{2anb\sin\theta}} \tag{10}$$

In the general case, the curved channel can be treated as consisting of various segments of variable length, width and orientation. We refer to a channel such that in each one of its segments, values of the width and orientation are kept constant. If the number of channel segments in which salinity is greater than the dilution value is J, then J can be determined by applying the following relationships:

$$\sum_{j=1}^{J}\left[\frac{q_a L_j}{Q_c}\sqrt{\frac{2anb_j \sin\theta_j}{n+1}}\right] \geq 4.6 \tag{11}$$

where j is the number of the particular channel segment; L_j is the length of the segment; θ_j is the orientation angle of the segment; and b_j is the width of the segment.

Any cross section of the curved channel, which is located upstream of the complete dilution point, represents an interface of direct contact between saline and freshwater. Downstream of the direct contact interface along the aquifer flowline, we calculate the variation of the salinity distribution in the overlying aquifer. Owing to the small length of the interface of direct contact the mineralized zone thickness is generally smaller than the aquifer thickness at the downstream edge of the channel, namely at $\xi = b/\sin\theta$. For large distances downstream of the direct contact interface, the mineralized zone may occupy the entire thickness of the aquifer. The following subsections refer to sections of the aquifer located downstream of the direct contact interface.

Section of δ_0-development

A mineralized zone with a height smaller than the aquifer thickness characterizes this section of the aquifer. Downstream of the direct contact interface, the boundary condition at the bottom of the aquifer changes from a constant salinity boundary to a vanishing salinity flux boundary. There is no more supply of salinity into the aquifer flowlines, but the salinity profile is subject to expansion due to dispersion. The mineralized zone occupies a portion of the aquifer, and the salinity profile consists of two BLs (Rubin and Buddemeier, 1998c), illustrated in Fig. 7. One

BL develops at the bottom of the aquifer and is termed the inner BL. The other one is termed the outer BL, and it develops on top of the inner BL. The thickness of the inner BL is δ_u.

We choose a normalized isohaline c_r, where c_r represents the ratio between the salinity of that particular isohaline and the salinity at the bottom of the aquifer. At the left-hand side of the downstream edge of the channel, where $\xi=b/\sin\theta$, we refer to the ordinate $z=\delta_u$ at which the salinity is $c_r C_c$. The normalized isohaline c_r represents the top of the inner BL. However, as shown in Appendix A, it is necessary to consider effects stemming from the variation of the salinity profile from a profile of constant salinity to a profile of no diffusive flux at the aquifer bottom.

Numerous numerical experiments were performed (Rubin and Buddemeier, 1998c) with regard to the BLs developed at the right hand side of the downstream edge of the channel. These showed that if the thickness of the mineralized zone, δ_0 is smaller than the thickness B, of the aquifer, and if c_r=0.5, then there is almost no salinity transferred between the inner BL and the outer BL.

The salinity distribution in the inner BL is given by:

$$C_a = C_b\left[1-(1-c_r)(1-\lambda)^{n_1}\right]; \quad \lambda = \frac{\delta_u - z}{\delta_u}; \quad 0 \le z \le \delta_u \tag{12}$$

where C_b is the contaminant concentration at the bottom of the overlying aquifer, n_1 is a power coefficient; λ is the inner BL coordinate.

The outer BL is represented by the following salinity profile:

$$C_a = c_r C_b (1-\zeta)^{n_2}; \zeta = \frac{z-\delta_u}{\delta_0 - \delta_u}; \delta_u \le z \le \delta_0 \tag{13}$$

where n_2 is a power coefficient; ζ is the outer BL coordinate, and δ_0 is the thickness of the portion of the aquifer subject to mineralization.

Many numerical experiments, performed by the authors (Rubin and Buddemeier, 1998c) have indicated that the following values are applicable:

$$n_1 = 1.84; \quad n_2 = 4 \tag{14}$$

The length of the portion of the overlying aquifer subject to mineralization consists of two regions: a) the steady state region, and b) the spearhead region. The length of the steady state region is approximately V_aT, where T is the time interval measured from the initial contact between the saline channel water and the freshwater of the overlying aquifer. The length of the spearhead region is equal to the length of the interface of direct contact between the channel and the overlying aquifer, namely $b/\sin\theta$. Due to the short length of the spearhead region, it has very small effect on the aquifer mineralization, and is neglected in our calculations.

Downstream of the downstream edge of the channel the values of δ_u and δ_0 are subject to development according to the following expressions:

$$\delta_u^2 = \left(\delta_u^2\right)_{\xi=b/\sin\theta} + \alpha_1 \frac{2a(1-c_r)n_1(n_1+1)}{n_1+c_r}\left(\xi - \frac{b}{\sin\theta}\right); \quad \frac{b}{\sin\theta} \le \xi \le V_aT - \frac{b}{\sin\theta} \tag{15}$$

$$(\delta_0 - \delta_u)^2 = (\delta - \delta_u)^2_{\xi=b/\sin\theta} + 2\alpha_2 a n_2(n_2+1)\left(\xi - \frac{b}{\sin\theta}\right); \quad \frac{b}{\sin\theta} \le \xi \le V_aT - \frac{b}{\sin\theta} \tag{16}$$

where α_1 and α_2 are constant coefficients. Numerical experiments and the principle of mass conservation can be used to determine their values. Such an approach yields (Rubin and Buddemeier, 1998c)

$$\alpha_1 = 0.935; \quad \alpha_2 = 0.775 \tag{17}$$

According to the principle of mass conservation:

$$C_b\delta_u = \left(C_b\delta_u\right)_{\xi=b/\sin\theta} \tag{18}$$

$$C_b\delta_0 = \left(C_b\delta_0\right)_{\xi=b/\sin\theta} \tag{19}$$

These expressions provide the value of C_b, and are also useful for the determination of the coefficients α_1 and α_2.

Only part of the mineralized zone thickness comprises the ROI (region of interest), which is the top specified boundary layer (TSBL). In the ROI the salinity is higher than the acceptable value C_T. Either one of the following expressions gives the thickness of the ROI:

$$\delta = \delta_u (1 - \lambda_T); \quad \lambda_T = 1 - \left[2\left(1 - \frac{C_T}{C_b}\right)\right]^{1/n_1} \tag{20}$$

$$\delta = \zeta_T (\delta_0 - \delta_u) + \delta_u; \quad \zeta_T = 1 - \left(\frac{C_T}{c_r C_b}\right)^{1/n_2} \tag{21}$$

The first expression is applicable if $\delta < \delta_u$. The second expression is applicable if $\delta > \delta_u$.

Due to the expansion of the mineralized zone, it approaches the top of the aquifer. At the attachment point, the mineralized zone reaches the top of the aquifer, and its thickness is identical to the aquifer thickness, B. The following subsection refers to sections of the aquifer located downstream of the attachment point.

The restructuring section

The restructuring section is located downstream of the attachment point. Two BLs of different thickness characterize the restructuring section. The inner BL develops in this section on account of the outer BL. The thickness of the inner BL is δ_u. We define two types of BL coordinates, referring to the inner and outer BL, respectively:

$$\lambda = \frac{\delta_u - z}{\delta_u}; \quad 0 \leq z \leq \delta_u \tag{22}$$

$$\zeta = \frac{z - \delta_u}{B - \delta_u}; \quad \delta_u \leq z \leq B \tag{23}$$

The salinity profiles of the inner and outer BLs are given, respectively by Rubin and Buddemeier (1998c):

$$\frac{C_a - C_t}{C_b - C_t} = 1 - 0.5(1-\lambda)^{n_3}; \quad 0 \le z \le \delta_u \tag{24}$$

$$\frac{C_a - C_t}{C_b - C_t} = 0.5(1-\zeta)^{n_4}; \quad \delta_u \le z \le B \tag{25}$$

where C_b and C_t represent the salinity at the bottom and top of the aquifer, respectively.

In order to comply with the conservation of mass, as shown in Appendix A, some adjustment of BL quantities should be made at the attachment point.

We define a longitudinal coordinate X, where X=0 represents the attachment point. The value of X associated with a given value of δ_u in the restructuring section is given by:

$$\gamma \frac{a n_1 x}{B^2} = -\beta_1 \left(\frac{\delta_u}{B} - \frac{\delta_{u0}}{B} \right) + \beta_2 \left[\left(\frac{\delta_u}{B} \right)^2 - \left(\frac{\delta_{u0}}{B} \right)^2 \right] - \beta_3 \ln \left[\frac{\beta_4 - \beta_5 \left(\frac{\delta_u}{B} \right)}{\beta_4 - \beta_5 \left(\frac{\delta_{u0}}{B} \right)} \right] \tag{26}$$

where β_i $(i = 1,\ldots5)$ are coefficients, whose values are given in Appendix B, and γ is a coefficient of calibration of the model. The numerical simulation results compared with the BL approach implies $\gamma \approx 2.5$ (Rubin and Buddemeier, 1998e). Rubin and Atkinson (1998) developed a power series expansion solution for a similar problem concerning effluent mixing in rivers.

At the downstream end of the restructuring section, the establishment point is where the inner BL thickness is equal to approximately half of the thickness of the aquifer. Introducing this value into eq. (26) yields the length of the restructuring section:

$$L_R = \frac{B^2}{\gamma a n_3} \left\{ -\beta_1 \left[\left(\frac{1}{2} \right) - \left(\frac{\delta_{u0}}{B} \right) \right] + \beta_2 \left[\left(\frac{1}{2} \right)^2 - \left(\frac{\delta_{u0}}{B} \right)^2 \right] + \beta_3 \ln \left[\frac{\beta_4 - \beta_5 \left(\frac{1}{2} \right)}{\beta_4 - \beta_5 \left(\frac{\delta_{u0}}{B} \right)} \right] \right\} \tag{27}$$

The salinities at the bottom and top of the aquifer in the restructuring section are given, respectively by:

$$C_b = \frac{C_{b0}}{2(n_3+0.5)(n_4+0.5)-0.5}\left[2(n_3+0.5)(n_4+0.5)\frac{\delta_{u0}}{\delta_u} - 0.5\frac{B-\delta_{u0}}{B-\delta_u}\right] \quad (28)$$

$$C_t = \frac{C_{b0}(n_3+0.5)}{2(n_3+0.5)(n_4+0.5)-0.5}\left[\frac{B-\delta_{u0}}{B-\delta_u} - \frac{\delta_{u0}}{\delta_u}\right] \quad (29)$$

where C_{b0} is the salinity of the aquifer bottom at the right hand side of the attachment point.

Numerical experiments and results obtained by Rubin and Buddemeier (1998e) suggest using the following values of the power coefficients:

$$n_3 = 1.5; \quad n_4 = 2.5 \quad (30)$$

The establishment section

In the establishment section there are two BLs, inner and outer BLs. The inner BL occupies the lower half of the aquifer thickness. The upper BL occupies the upper half of the aquifer thickness. Salinity profiles in the inner and outer BLs are given by eqs. (24) and (25), respectively, while considering that $\delta_u = B/2$. However, in the establishment region, both BLs have the identical power coefficient n_5. Therefore some adjustment should be made to the values of C_b and C_t, to comply with the principle of mass conservation, as shown in Appendix A.

At the downstream end of the establishment section, the difference in salinity between the top of the aquifer and its bottom is very small; an appropriate definition should be adopted for "very small". We assume that the salinity profile is uniform if the difference between C_b and C_t is smaller than 1%. The uniformity point represents the downstream end of the establishment section.

The length L_E of the establishment section is given by:

$$L_E = \frac{B^2}{8\alpha_3 a n_5} \ln\left[100(C_b - C_t)_{es}\right] \tag{31}$$

where α_3 is a constant coefficient; the subscript *es* refers to the right hand side of the establishment point (see Fig. 7); n_5 is the power coefficient of the establishment section. Its value is about n_5= 1.8. The value of the coefficient α_3, according to numerical experiments (Rubin and Buddemeier, 1998e), is about 0.6.

Values of C_b and C_t at the right hand side of the establishment point are obtained by applying the principle of mass conservation, as shown in Appendix A

The salinities at the bottom and top of the aquifer in the establishment section are given, respectively, by:

$$C_b = \frac{1}{2}\left[(C_b + C_t)_{es} + (C_b - C_t)_{es} F\right] \tag{32}$$

$$C_t = \frac{1}{2}\left[(C_b + C_t)_{es} - (C_b - C_t)_{es} F\right] \tag{33}$$

where

$$F = \exp\left[-\alpha_3 \frac{8an_5}{B^2}(X - L_R)\right] \tag{34}$$

WINDING CHANNEL

All basic equations and expressions developed for the curved channel are also applicable to portions of the winding channel that are in contact with approaching fresh groundwater of the overlying aquifer. We can also apply expressions referring to portions of the aquifer located downstream of the interface of direct contact between the saline water of the channel and groundwater of the overlying aquifer. Differences between calculations referring to curved and winding channels originate from direct contact between the channel saline water and groundwater of the overlying aquifer which is already mineralized. There are also possibilities for salinity transfer from the mineralized aquifer into the channel, provided that the direct contact interface is located downstream of the complete dilution point of the channel. However, salinity values of the approaching groundwater are usually small, and we ignore such phenomena. Our analysis and calculations refer to the portion of the channel, which is located upstream of the point of complete dilution.

Calculations for the curved channel case which refer to sections of the aquifer downstream of the interface of direct contact are also applicable to winding channel calculations.

For interfaces of direct contact between the channel saline water and mineralized groundwater of the overlying aquifer, the calculation of C_c can be performed according to eq. (4), without the simplification of eqs. (7) and (9). Interfaces of direct contact, between the channel saline water and mineralized groundwater of the aquifer, may follow either one of the sections which characterize the mineralized portion of the aquifer.

An approaching mineralized groundwater front has the shape of a spearhead whose length is equal to $b/\sin\theta$, where b and θ refer to the last direct contact interface, in which the aquifer water was subject to mineralization. However, the spearhead region is comparatively small, and we neglect phenomena associated with this region. The steady state region of the approaching mineralized aquifer water may occupy a portion of the thickness of the aquifer, or the entire thickness of the aquifer, as shown in Figs. 6, 7, and 8. In both cases, the approaching salinity profile incorporates two BLs. As it moves over the direct contact interface, the salinity profile is subject to an abrupt change in the bottom boundary condition which leads to restructuring of the salinity profile as a single BL. Calculations of this restructuring process are based on the principle of mass conservation, as shown in Appendix A.

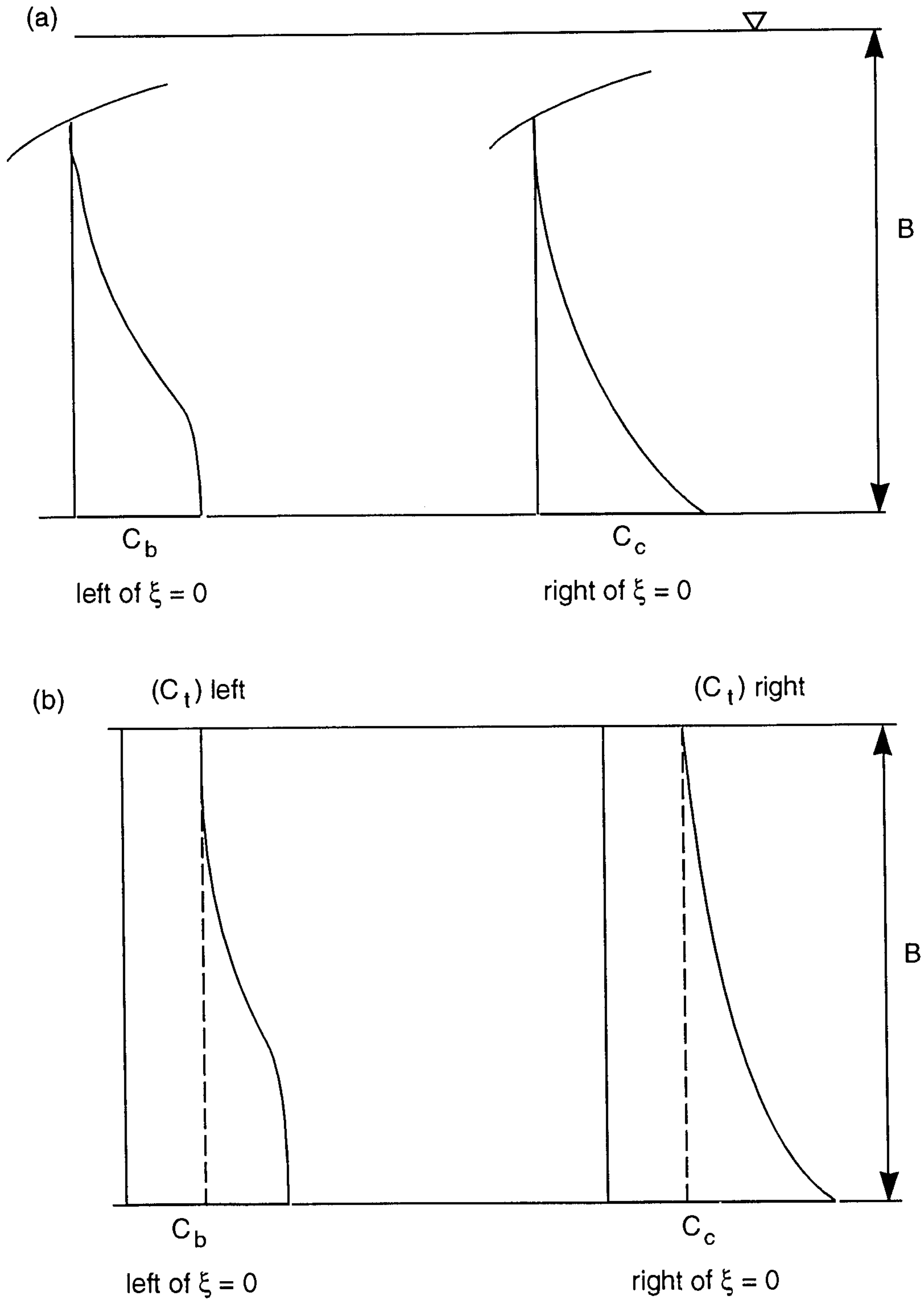

Fig.8 Restructuring of the salinity profile at the downstream edge of the channel (ξ=0) of a winding channel

(a) Mineralized zone thickness is smaller than the aquifer thickness, B

(b) Mineralized zone thickness occupies the entire thickness of the aquifer

If the adaptation of the salinity profile at the upstream edge of the channel(ξ=0) creates a mineralized zonewith a thickness smaller than the thickness of the aquifer then the salinity profile built on top of the direct contact interface is represented by eq. (5). At the downstream edge of the channel, where $\xi = b/\sin\theta$, the thickness of the mineralized zone is given by:

$$\left(\delta_0^2\right)_{\xi=b/\sin\theta} = \left(\delta_0^2\right)_{\xi=0} + 2an(n+1)b/\sin\theta \tag{35}$$

We introduce the expressions for the salinity profiles in eq. (4), to obtain:

$$\frac{dC_c}{C_c} = -\frac{q_a \sin\theta}{Q_c(n+1)}\left[\left(\delta_0\right)_{\xi=b/\sin\theta} - \left(\delta_0\right)_{\xi=0}\right]dx' \tag{36}$$

By direct integration of eq. (36) we obtain:

$$\ln\left(\frac{C_c}{C_{c0}}\right) = -\frac{q_a \sin\theta}{Q_c(n+1)}\int_0^{\Delta x'}\left[\left(\delta_0\right)_{\xi=b/\sin\theta} - \left(\delta_0\right)_{\xi=0}\right]dx' \tag{37}$$

If there is a minor difference between the thickness of the mineralized zone at the downstream and upstream edges of the channel then eq. (37) can be approximated by:

$$\ln\left(\frac{C_c}{C_{c0}}\right) = -\frac{q_a anb}{Q_c}\int_0^{\Delta x'}\frac{dx'}{\left(\delta_0\right)_{\xi=0}} \tag{38}$$

It should be noted that in the winding channel case, the intensity of salinity transfer from the channel flow into the aquifer per unit channel length is smaller than in the curved channel case with identical values of b and θ. Therefore, the complete dilution length L_D of a winding channel is longer than that of a curved channel.

At the downstream edge of the channel the salinity profile should accommodate to the abrupt change in the bottom boundary condition, as discussed in Appendix A.

If the mineralized zone of the approaching groundwater occupies the entire thickness of the aquifer, as shown in Fig. 8(b), then the salinity profile of the approaching mineralized groundwater consists of two BLs. In this case the salinity profile can be expressed by eqs. (24) and (25), provided that the approaching salinity profile is typical of the restructuring section (see

Fig. 7). Equations (24) and (25) are also applicable with n_5 replacing n_3 and n_4 if the approaching salinity profile is representative of the establishment section.

Owing to the abrupt change in the bottom boundary condition of the salinity profile at the upstream edge of the channel, the profile of two BLs is adapted to a salinity profile of a single BL. If the resulting single BL occupies the entire thickness of the aquifer then the salinity profile of this BL is given by:

$$C_a = C_t + (C_c - C_t)(1-\omega)^{n_6} \tag{39}$$

where n_6 is a power coefficient, and ω is the BL coordinate, which is given by:

$$\omega = \frac{z}{B} \tag{40}$$

In order to determine the appropriate value of the power coefficient n_6 of eqs. (39), we apply the analytical solution for an analogous problem of heat conduction in solids. For the overlying aquifer under steady state conditions, the equation of dispersion-advection yields approximately:

$$\frac{\partial C_a}{\partial x} = a\frac{\partial^2 C_a}{\partial z^2} \tag{41}$$

This equation is subject to the following boundary conditions:

$$\begin{aligned} C_a &= C_c \quad at \quad z=0 \\ \frac{\partial C_a}{\partial z} &= 0 \quad at \quad z=B \\ \frac{\partial C_a}{\partial x} &= 0 \quad at \quad x \to \infty \end{aligned} \tag{42}$$

Equation (41) subject to the boundary conditions of eq. (42) is completely analogous to the problem of build-up of the temperature profile in a solid bounded by two parallel planes, where one end is kept at constant temperature and the other end is insulated. The analytical solution to this problem is given by Carslaw and Jaeger, (1959). Their solution implies for our case:

$$\frac{C_a}{C_c}=1-\frac{4}{\pi}\sum_{m=0}^{\infty}\frac{1}{2m+1}\exp\left[-\frac{(2m+1)^2\pi^2 ax}{4B^2}\right]\sin\left[(2m+1)\frac{\pi z}{2B}\right] \tag{43}$$

The BL approximate salinity profile represented by eq. (39) can be introduced into eq. (41). Then by using Leibniz's theorem and performing integration of the expressions we obtain the following expression for the calculation of C_t:

$$\ln\left(\frac{C_c-C_t}{C_c}\right)=-\frac{a(n_6+1)x}{B^2} \tag{44}$$

In order to find the appropriate value of n_6, we have performed calculations of salinity profiles for various values of x by applying eqs. (39) and (44), as well as by using eq. (43). We found that about 6 terms are needed to obtain practically complete convergence of the series expansion shown in eq. (43). Figure 9 shows some examples of our simulations for comparatively large x-values. This figure refers to a = 0.1 m, B = 40 m, and two possible values of n_6 = 1.2, and 1.8. It seems that for small values of x the series expansion solution of eq. (43) is not accurate, and can be replaced by the complementary error function solution, which is typical of semi-infinite domain. Under such conditions the value of n_6 can be replaced by n, namely 3. For large values of x, smaller values of n_6 should be considered. However, we may assume that values between 1.2 and 1.8 are satisfactory. Only minor errors are introduced into the calculation by considering a constant value of n_6 for the entire domain.

At the downstream edge of the channel the salinity profile should again be subject to some adjustments. Possible adjustments of the salinity profiles at that location are given in Appendix A.

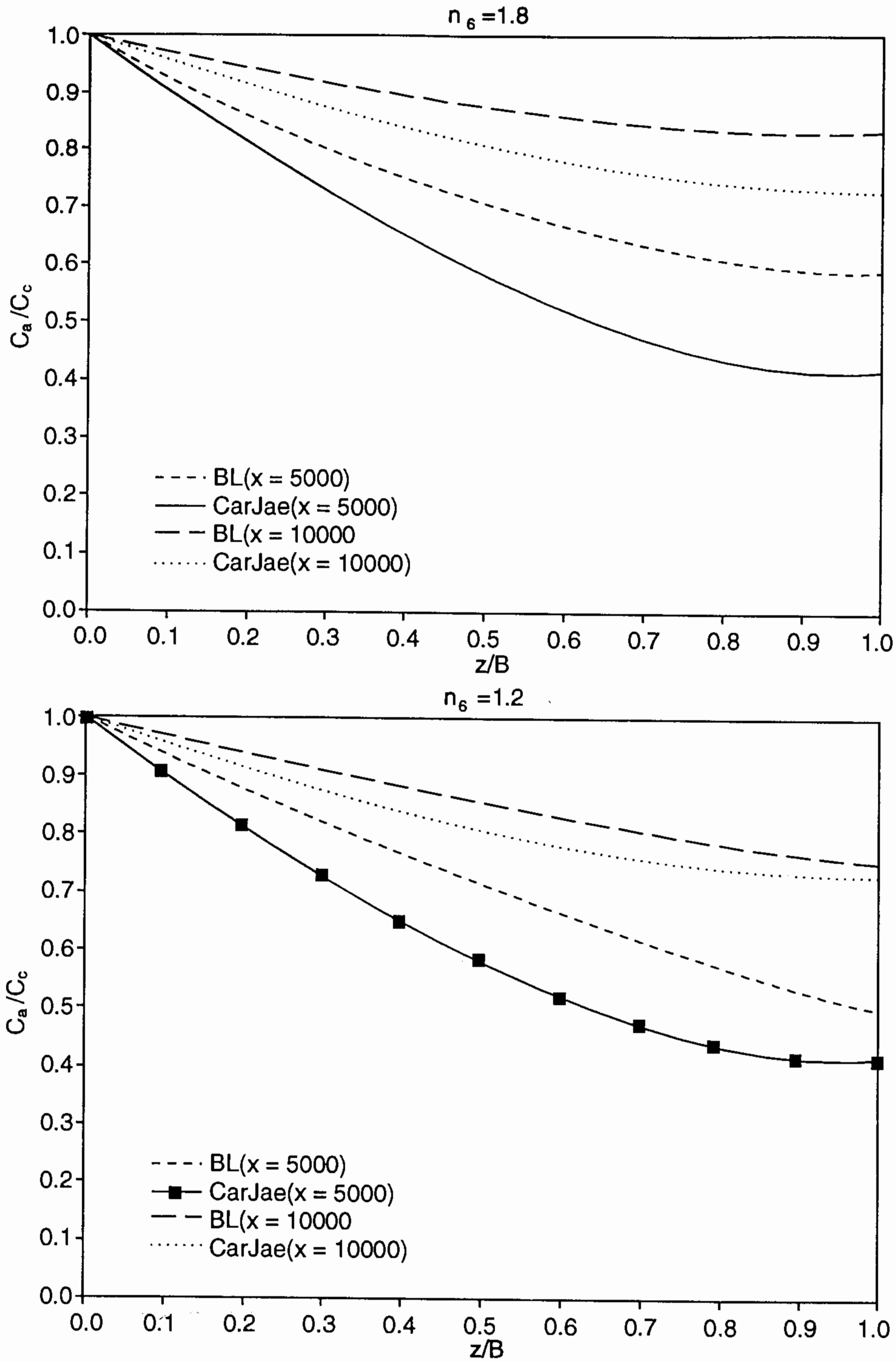

Fig. 9 Comparison between the BL solution and the analytical solution (Carslaw and Jaeger, 1959) for mineralized zone build-up, above the direct contact interface, in the entire thickness of the aquifer

(a) $n_6 = 1.8$

(a) $n_6 = 1.2$

PRACTICAL USE OF THE METHOD

This section provides an example of the practical use of the method developed in this study. We analyzed the mineralization induced in the Great Band Prairie aquifer of south central Kansas, by a saline-water channel illustrated in Figure 10. Measurements of potentiometric heads in the overlying aquifer during 1996 provide contours of the potentiometric heads, which are shown with 20 ft intervals in that figure. We used potentiometric head contours, to depict flowlines of the aquifer flow in the region subject to mineralization by the saline water flowing through the channel. Along each flowline, calculations of the build-up and spatial variation of the salinity profile were performed. We provide details about variations of salinity along the course of the channel flow until complete dilution is obtained. Along the aquifer flowlines, complete dilution or uniformity of the salinity profile represents the point of uniformity. With regard to the aquifer mineralization process, we provide details of calculations referring to a single flowline. Calculations regarding other flowlines are similar. We refer to the flowline, marked by A in Fig. 10, shown as originating near the salinity source in that figure. Along this flowline numbers represent successive segments of 1 km. This flowline crosses the channel at the point of direct contact with the bedrock source of the saline water. Along the channel, as along the flowline, numbers show segments of 1 km length.

The average hydraulic gradient along the aquifer flowlines is about 0.33%. For the first portion (about 12 km) of the channel, the hydraulic gradient along the channel course is about 0.2%. According to the schematic of Fig. 3, we assume an average width and depth of the channel of 30 m and 5 m, respectively. Therefore the cross section area of the channel is about 150 m^2. We also assume that the channel width at the interface of direct contact ($b\sin\theta$) is about $b = 50$ m. The channel hydraulic conductivity is taken as K_c, = 500 m/d. Therefore, we obtain a channel flow-rate of about $Q_c = 150$ m^3/d. The hydraulic conductivity of the aquifer is assumed to be about $K_a = 10$ m/d. Therefore the specific discharge of the aquifer flow is $q_a = 3.3\times10^{-2}$ m/d.

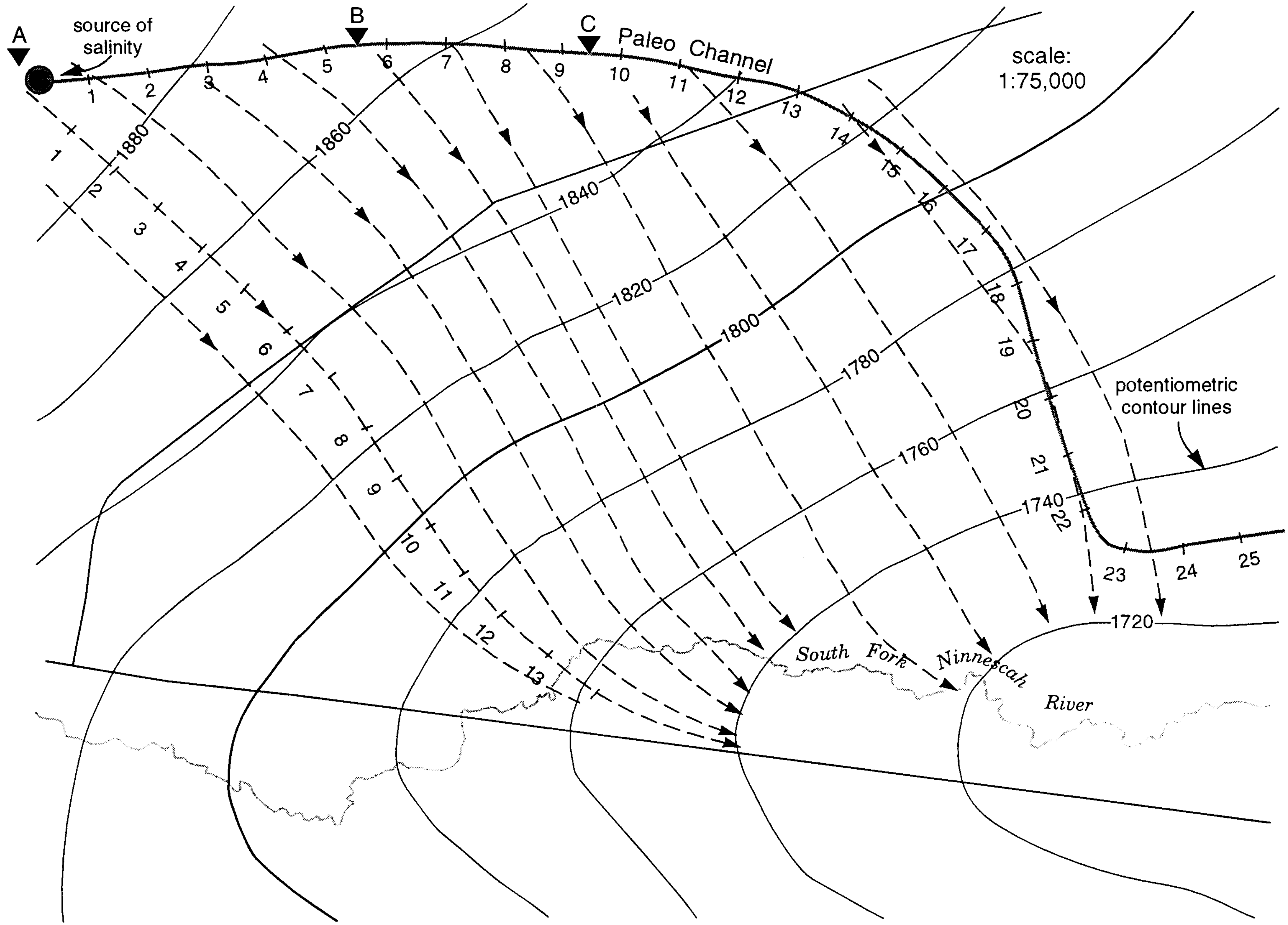

Fig. 10 A specific channel with an assumed salinity source and flowlines of the overlying aquifer indicated. Distances in km are indicated along the channel and the flowline, marked by A and used for sample calculations. Points A, B, and C represent the contact locations for the sample calculation flow line (on which C_{av}=0.025 C_{c0}) and the flowlines with C_{av}=0.01C_{c0} and C_{av}=0.005 C_{c0}, respectively.

Along the first 12 km of the channel, its angle of orientation to the aquifer flowlines is about $\theta = 50^0$. Considering an aquifer dispersivity of $a = 0.1$ m, we introduce values of the appropriate parameters into eq. (10) to obtain a dilution length of the channel of about $L_D =$ 8700m. However, the study of Garneau (1995) suggests considerably smaller values of the aquifer dispersivity. If $a = 0.052$ m, then the dilution length is about 12 km. For smaller values of the dispersivity we have to take into account the variation of the channel orientation and use eq. (11). If we assume that $a = 0.01$ m, then the channel is defined as a winding channel. For such a small dispersivity value the channel segments between points of 17km and 24km are approached by aquifer groundwater that is mineralized by previous segments of the channel. If we assume that the South Fork Ninnescah River gets some saline water from the mineralized portion of the aquifer, our calculation with regard to salinity profile variations in the flowline considered in Fig. 10 can be applicable up to a distance of 13 km downstream of the salinity source, where the aquifer flowline reaches the river. The method of this paper can be applied to calculations of salinity transport downstream of the river provided that some more information about salinity discharge into the river becomes available. Our calculations use $a = 0.01$ m; however, they can easily be modified with other values for dispersivity to study the sensitivity of the physical phenomenon to this parameter.

By applying eq. (6), we obtain $\delta_0 = 3.95$ m, $\delta_u = 0.82$ m as values for the mineralized zone and inner BL thicknesses, respectively, at the downstream edge of the channel ($\xi = b/\sin\theta$). By applying eqs. (15) and (16), we find that the attachment point (see Fig. 7) is located at ξ=3200 m. The salinity at the bottom of the aquifer at that location is about 10% of the channel salinity at its entrance. At the attachment point, the thickness of the inner BL is modified as indicated by Appendix A and changes from $\delta_u = 8.2$ m to $\delta_u = 11.4$ m. By applying either eq. (20) or eq. (21), we obtain the value of the ROI thickness. If we consider that $C_T = 0.01C_{c0}$, where C_{c0} is the salinity at the entrance of the channel, then we obtain $\delta = 32.1$ m. Considering that we use a value of $B = 40$ m for the aquifer thickness, the resulted value of δ indicates that although the entire thickness of the aquifer is mineralized at the attachment point, at the top 8m of the aquifer, groundwater is practically fresh. By applying eqs. (28) and (29), we calculate values of the salinity at the top and bottom of the aquifer at the establishment point. We find that C_b is about 4% of the channel entrance salinity, and C_t is about 1.1% of the channel entrance salinity. Considering that acceptable salinity is 1% of the channel entrance salinity, our result indicates that at the establishment point the aquifer is completely mineralized.

By applying eq. (27) we obtain a restructuring length of about L_R = 6000 m. This result indicates that when the sample flowline intersects the South Fork Ninnescah River its salinity profile is in the establishment section (see Fig. 7). However, only about 4000 m of that region can practically be considered, as the distance between the channel entrance and the river measured along the aquifer flowline, is about 13.2 km and the attachment point is at 3200 m downstream of the channel. Nonetheless, we applied eqs. (31)-(34) and calculated variations of the salinity profile until achieving the hypothetical condition of uniformity, in which difference of salinity between bottom and top of the aquifer is smaller than $0.01C_{c0}$. By applying eq. (31), and ignoring any effect of the South Fork Ninnescah River, we obtain the length of the establishment section as L_E = 20 km. Equations (34) and (35) indicate that at the downstream end of the establishment section, the salinity distribution is practically uniform, and its value is about 2.4% of the salinity of the channel flow at its entrance. This is, of course, the value of the average salinity of the flowline. However the establishment section calculations are relevant only up to the point of the South Fork Ninnescah River, at which values of the salinity at the bottom and top of the aquifer are about 3.7% and 1.4%, respectively, of the salinity at the entrance of the channel. At that point, probably substantial quantities of the groundwater flow into the South Fork Ninnescah River. Simulation of mineralization characteristics of the flowline considered in Fig. 10, can easily be adapted for neighboring flowlines. In Figs. 11 - 14, we provide details of such simulations and their implications.

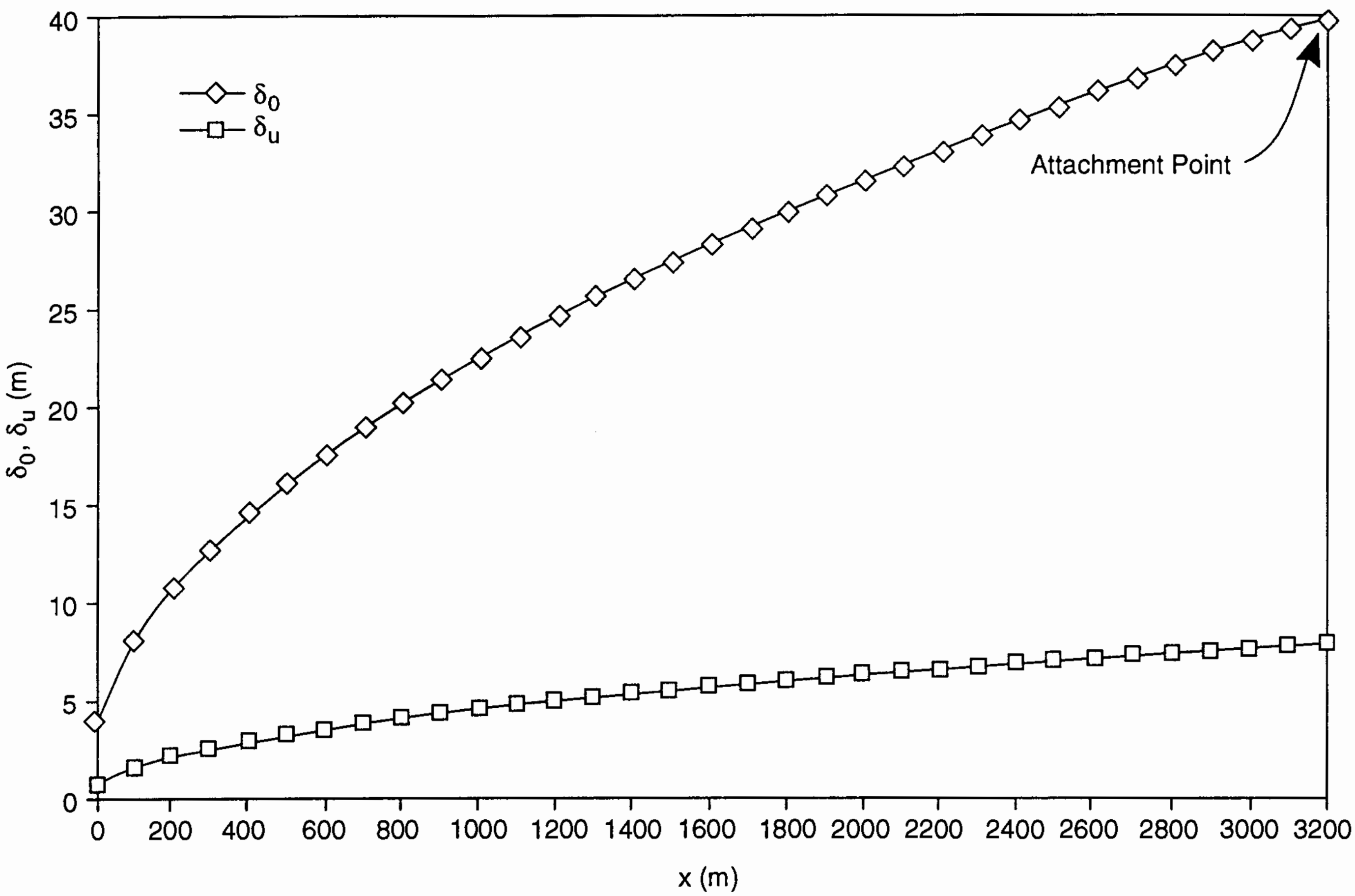

Fig. 11a Variations of the mineralization zone characteristics at the section of δ_0-development along the sample calculation flowline, shown in Fig. 10, and marked by A.

(a) Growth of δ_0 and δ_u until δ_0 =B

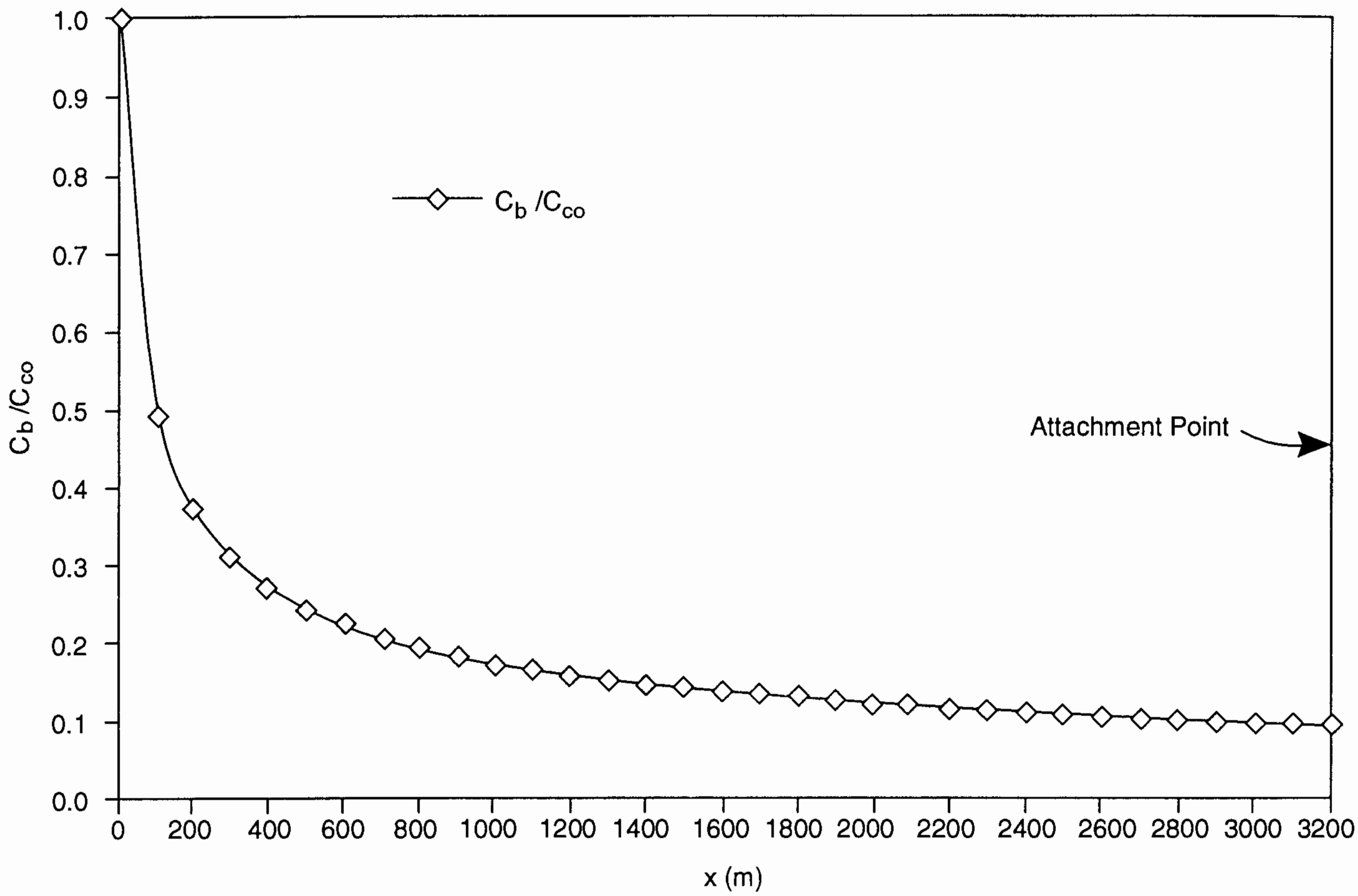

Fig. 11b Variations of the mineralization zone characteristics at the section of δ_0-development along the sample calculation flowline, shown in Fig. 10, and marked by A.

(b) Variation of C_b

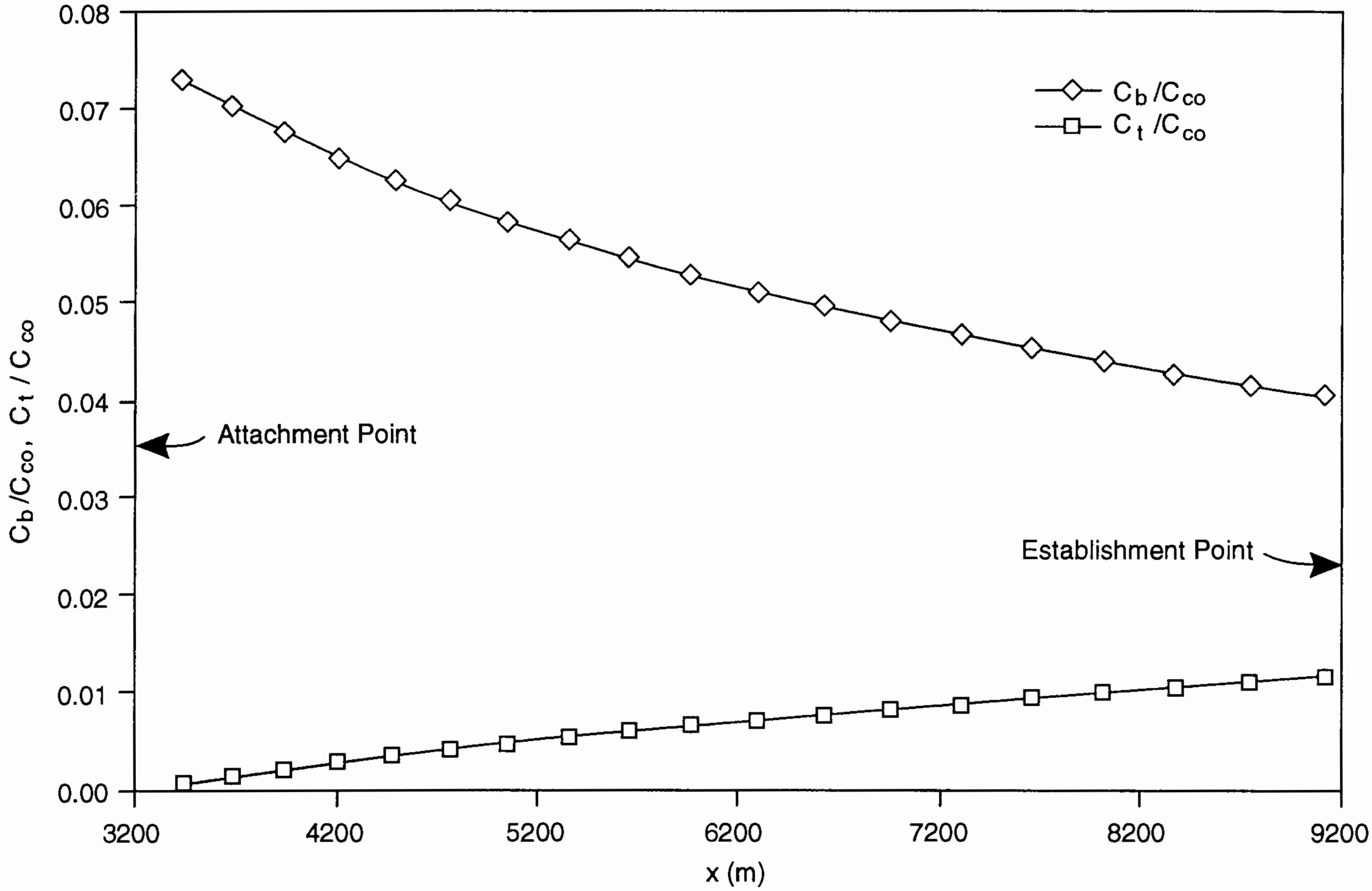

Fig. 12a Variations of the mineralization zone characteristics at the restructuring section along the sample calculation flowline shown in Fig. 10, and marked by A.

(a) Variation of C_b and C_t

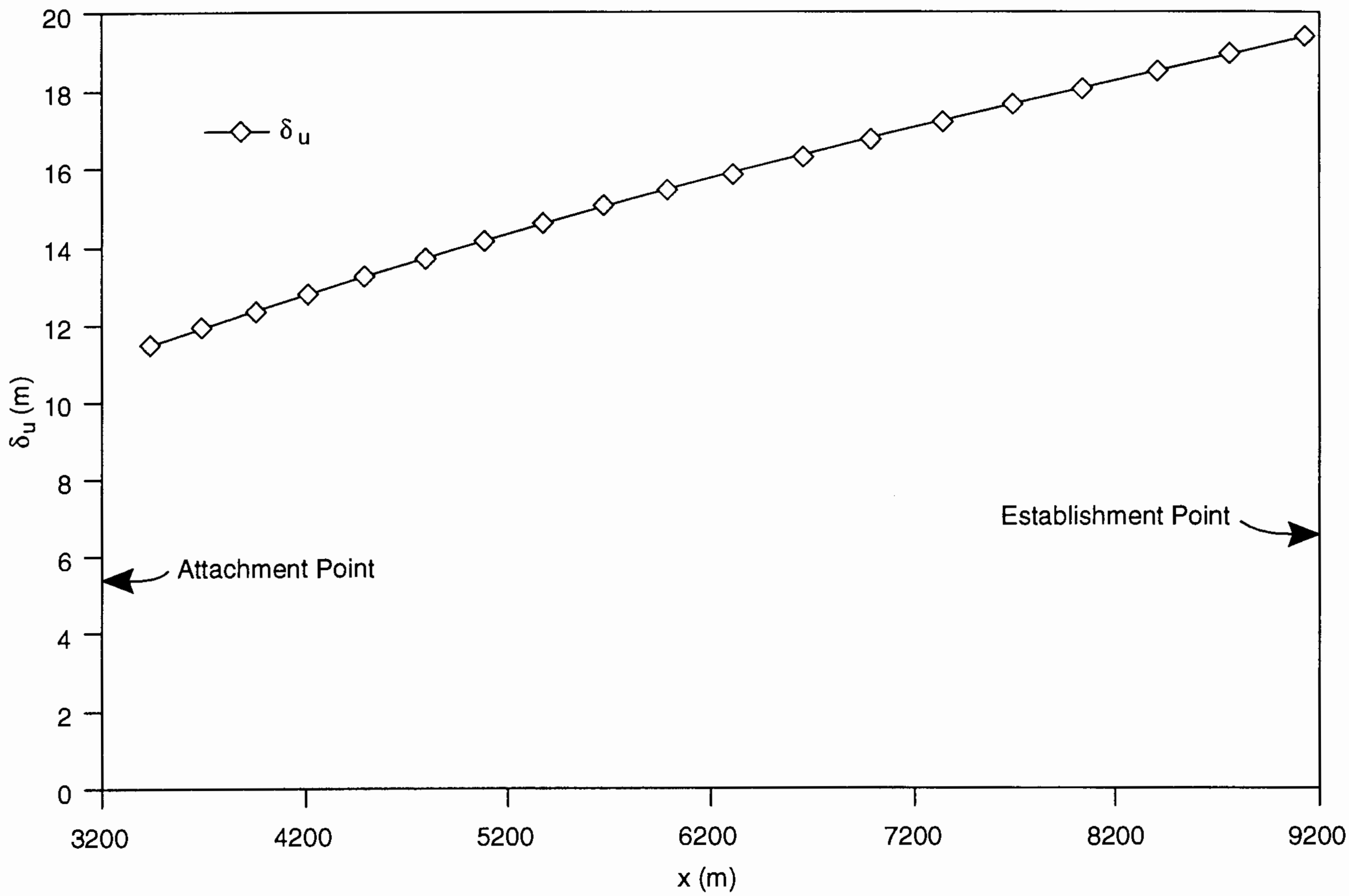

Fig. 12b Variations of the mineralization zone characteristics at the restructuring section along the sample calculation flowline shown in Fig. 10, and marked by A.

(b) Development of δ_u

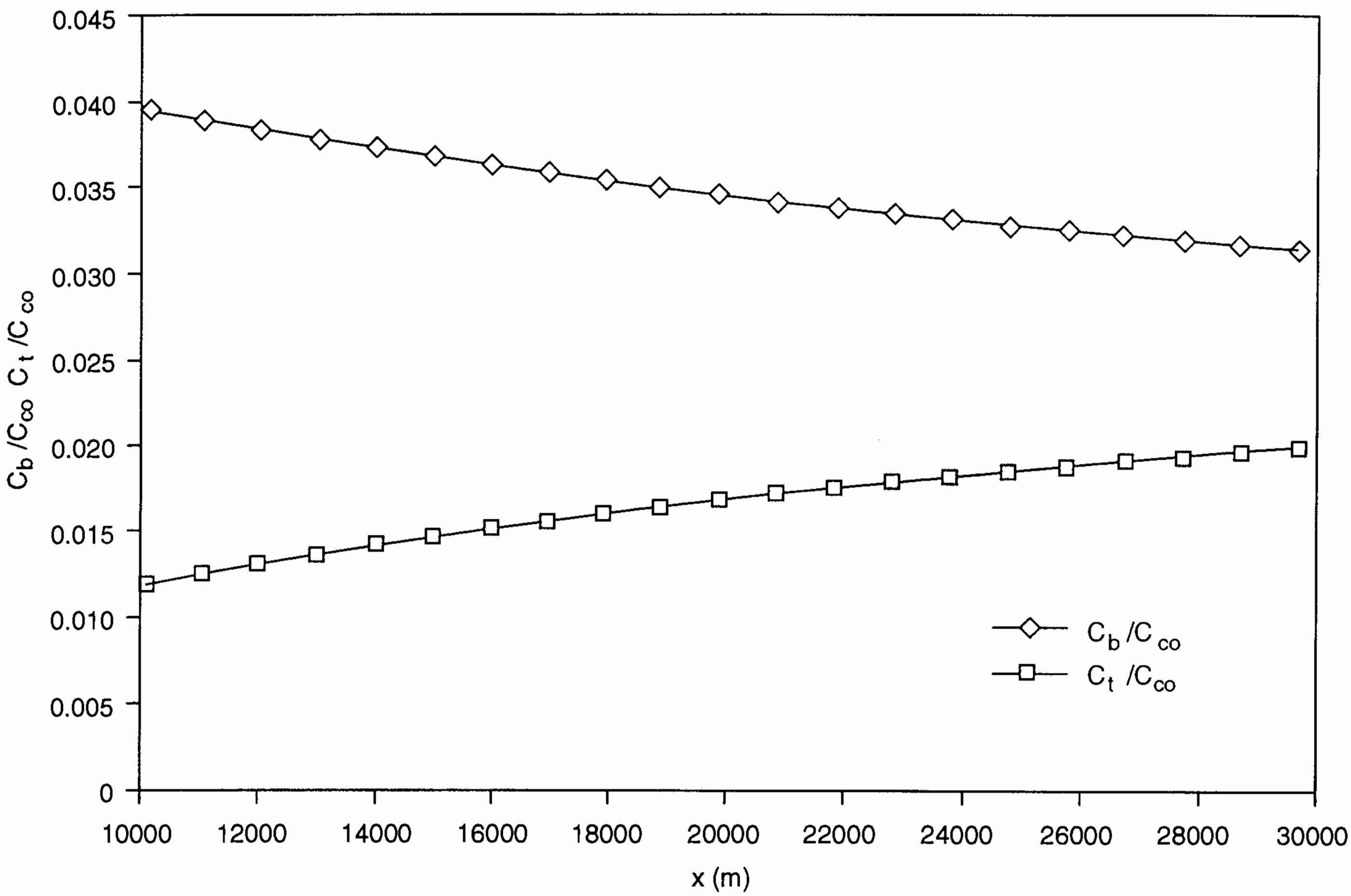

Fig. 13 Variation of C_b and C_t in the establishment section of the salinity profile along the sample calculation flowline shown in Fig. 10, and marked by A.

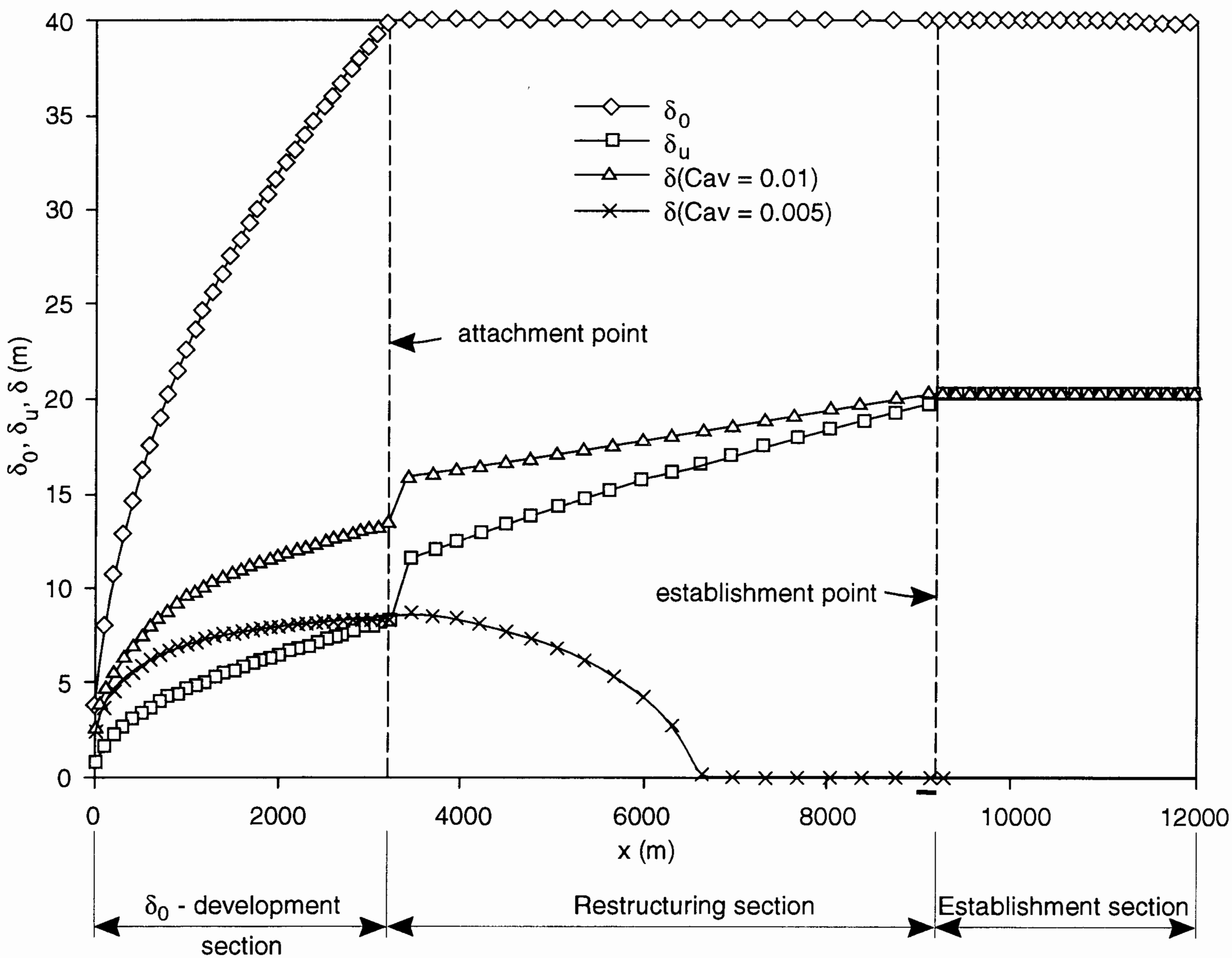

Fig. 14 Development of inner and outer BLs in the entire simulated domain and of the ROIs (δ) for the flowlines B ($C_{av} = 0.01$) and C ($C_{av} = 0.005$) for the system shown in Fig. 10.

Figure 11(a) describes the growth of the inner BL and the mineralized zone at the section of δ_0 development. The coordinate x, refers to distance from the downstream edge of the channel measured along the flowline. Figure 11(b) shows the variation of the salinity at the bottom of the aquifer. The value of C_b/C_{c0} in this figure represents the salinity at the bottom of the aquifer normalized with regard to C_{c0}. Figure 12(a) refers to the restructuring section. It shows the variation of the normalized salinity at the top and bottom of the aquifer. Figure 12(b) also refers to the restructuring section. It shows the moderate rate of growth of the inner BL, until its thickness occupies the lower half of the aquifer. Figure 13 refers to the establishment section. It indicates that the normalized value of C_b decreases and that of C_t increases, until they become almost identical. However, owing to the very small vertical salinity gradients in the aquifer cross section, complete uniformity of the salinity profile may be reached only at a very large distance downstream of the channel.

Calculations of the thickness of the various BLs, as well as calculations of values of C_b and C_t normalized with regard to C_c, are not affected by the value of C_c. However, the thickness δ, of the ROI is determined according to the definition of an acceptable value of salinity, C_T. We assume that $C_T = 0.01 C_{c0}$.

We identify aquifer flowlines, which carry salinity greater than C_T indefinitely and those carrying it only a limited distance along their course. The selection of the different types of flowlines depends on the average salinity of the flowline. This quantity is obtained by dividing the total salinity present at the aquifer cross section per unit width of the aquifer, by the aquifer thickness. This quantity is kept constant along the aquifer flowline. We may integrate the salinity profile over the aquifer thickness at the downstream edge of the channel to obtain the following expression for the average salinity of the flowline:

$$C_{av} = \frac{1}{B}\frac{\delta_0 C_c}{n+1} \tag{45}$$

By applying eqs. (45), (6) and (9), it is possible to identify the channel cross section associated with the production of a particular value of C_{av}. Such a cross section is located at a distance L_c from the channel entrance, where L_c is measured along the channel centerline. Its value is given by:

$$L_c = -\frac{Q_c}{q_a}\sqrt{\frac{n+1}{2anb\sin\theta}}\ln\left(\frac{C_{av}B}{C_{c0}}\sqrt{\frac{n+1}{2anb/\sin\theta}}\right) \tag{46}$$

Flowlines with an average salinity larger than C_T convey saline water indefinitely. A flowline with average salinity smaller than C_T, conveys saline water along a portion of its course. The average salinity of the flowline marked by A in Fig. 10 is about $0.025C_{c0}$, so it conveys saline water indefinitely. It should be noted that along the course of the flowline marked by A, there is no input or output of salinity. So the average salinity along that aquifer flowline is constant. We refer to two other flowlines of Fig. 10: the flowline with average salinity $C_{av} = 0.01C_{c0}$, and the flowline with average salinity $C_{av} = 0.005C_{c0}$. The first flowline, marked by B, according to eq. (46), crosses the channel at a distance of 5500 m downstream from the channel entrance. The latter flowline, marked by C, crosses the channel at a distance of 9600 m downstream. In Fig. 14, we depict the variation of the ROI thickness (δ) along these two flowlines. It should be noted that the value of δ, associated with $C_{av} = 0.01C_{c0}$, may represent the thickness of the portion of the mineralized zone, bounded by the isohaline at which $C_a = C_{av}$ for all flowlines in proximity to the channel entrance. As Fig. 14 covers a significant portion of the course of the aquifer flowlines, the adaptation of values of δ_u and thereby, also δ, at the attachment point is clearly shown in this figure. Figure 14 shows that along the first 6.3 km of the flowline of $C_{av} = 0.005C_{c0}$ saline water saturates a layer whose maximum thickness is about 8.6m. The flowline of $C_{av} = 0.01C_{c0}$ represents the boundary between flowlines that are indefinitely saline, and those that become practically fresh in a finite distance downstream of the channel.

DISCUSSION

Figs. 10 - 14 and the calculations and results of the preceding sectiondemonstrate that the major parameters which determine the characteristics of the channel mineralization process are: (a) the ratio between the specific discharge of the aquifer and the channel flow-rate, (b) the width of the channel, (c) the orientation of the channel, and (d) the dispersivity of the aquifer. Quantifications of the effect of each one of these parameters are given. Also the sensitivity of the mineralization process to changes of each parameter is easily inferred by the reference to the relevant analytical expressions obtained in the present study.

In various following paragraphs we refer to the concept of a stream tube, which represents the three-dimensional volume of the aquifer subject to flow. This volume is comprised of and bounded by streamlines. The stream tube can be represented by a vertical cross section of the aquifer, considered as a flowline in the present study. The present study considers the flowline and the salinity profile as two-dimensional representatives of the stream tube and its transverse average salinity profile.

The width of the channel and its orientation determine the length of the interface of direct contact, which is the distance along which salt is transferred from the channel into the overlying aquifer stream tubes. The dispersivity of the aquifer is a measure of the capability of the aquifer to obtain salinity from a unit length of the interface of direct contact. For small values of the orientation angle the interface of direct contact is long, but larger portions of the channel are subject to contact with mineralized groundwater. Therefore, as indicated by eq. (10), small orientation angles lead to longer dilution length of the channel. In cases of large orientation angle, approaching 90^0, there is probably a relatively small hydraulic gradient along the channel, so that the channel flow-rate is diminished, and saline water probably cannot be transported through the channel over long distances.

Large width of the channel increases the size of the interface of direct contact and intensifies the salinity transfer from the channel to the aquifer, so the dilution length is reduced.

An increase of the dispersivity intensifies the salinity transfer from the channel into the aquifer, reducing the dilution length of the channel. For a channel of constant width and orientation, the dilution length is inversely proportional to the value of the dispersivity. Our calculations indicate that for the particular channel of Fig. 10 and $a = 0.1$ m, the dilution length is about 8700 m. On the other hand for $a = 0.01$ m, the channel becomes a winding channel, and its dilution length becomes larger than 30 km. Therefore, in Fig. 10, a comparatively large portion of the aquifer is subject to mineralization if the dispersivity is small. However, in such a case, comparatively minute quantities of salt are transferred to each stream tube of the aquifer, and the mineralized stream tubes have low average salinity. Therefore, for a significant number of stream tubes located upstream of the point of complete dilution of the channel flow, the average salinity is low. Such stream tubes convey saline water comparatively short distances from the channel. In cases of high dispersivity the number of such stream tubes is comparatively small, as is the total number of aquifer stream tubes subject to mineralization. However, the majority of the mineralized stream tubes contain significant amounts of salinity, and in such stream tubes the salinity is high along the entire course of the aquifer flowlines.

Parameters of the channel and the aquifer, mentioned in the preceding paragraphs, determine how the flux of salinity is transferred to the aquifer stream tubes, and how the salinity is finally distributed in the aquifer, which is subject to mineralization. If we consider a stream tube of a specified width, there are two major options for mineralization of the aquifer stream tubes: (a) significant mineralization of a small number of stream tubes, and (b) minor mineralization of many stream tubes. The first option creates mineralized stream tubes, the majority of which carry salinity along their entire course. The latter option creates many mineralized stream tubes that carry salinity to a limited length of their course.

Our calculations basically assume that there are only minor changes in the streamline pattern. However, significant changes may be imposed due to seasonal variations originating from natural causes and artificial pumping. If changes are significant they may affect the distribution and direction of advection of the salinity in the aquifer, and should be taken into account.

SUMMARY

Groundwater mineralization may occur as a result of the flow of saline water in small bedrock channels with high permeability. Brines originating from deep saline bedrock formations mineralize these channel formations. The mineralization phenomenon was analyzed by applying the conceptual approach of the top specified boundary layer (TSBL). It is assumed that the salinity profile developed in the aquifer may consist of one or two boundary layers (BLs). Salinity is transferred from the channel into the aquifer through interfaces of direct contact between the channel flow and the aquifer flowlines. A single BL can represent the salinity profile developed on top of the interface of direct contact. Downstream of the channel edge, the salinity profile consists of two BLs, an inner and an outer BL. The salinity profile is subject to changes originating from the salinity distribution and the boundary conditions imposed by the top and bottom of the aquifer. Several different aquifer sections are identified, to characterize variations in the salinity profile along the course of the aquifer flowline. In the first section of δ_0-development, the mineralized zone thickness is smaller than the thickness of the aquifer. The following section is termed the restructuring section. It has a mineralized zone that occupies the entire thickness of the aquifer, but an expanding inner BL that is less than half of the aquifer thickness. In the final section, termed the establishment section, each of the BLs occupies half of the aquifer thickness, and their salinity values gradually become identical. Characteristic expressions were developed for the calculation of salinity transport and development of the BLs in the different sections of the aquifer.

We identify two general cases of channels: (a) curved channels, and (b) winding channels. Curved channels transfer salinity only to approaching freshwater of the overlying aquifer. Winding channels transfer salinity to both fresh and mineralized approaching groundwater.

Appropriate expressions were developed for the quantification of the salinity transfer from each type of channel to the aquifer flowlines.

The applicability of the method of analysis and calculation is exemplified by calculations relevant to a particular scenario of channel mineralization in south central Kansas. By applying the quantitative results of this example, major parameters of the mineralization process have been identified. It was shown that the channel might supply significant quantities of salinity to small number of stream tubes of the aquifer, or minute quantities of salinity to a comparatively large number of stream tubes. The outcomes of these two options are discussed.

Acknowledgement - This work was supported under contracts between the Kansas Water Office and the Kansas Geological Survey. The authors thank Marios Sophocleous and David Young for valuable comments and information. The authors are grateful for the assistance of Mark Schoneweis in preparing the illustrations.

Appendix A: Adjustment of BL quantities at points of interface between adjacent ranges of *x*-values

Compliance with the principle of mass conservation requires that some adjustment be made to values of quantities associated with the development of the various BLs in the simulated domain. Such adjustment is needed whenever the general equations describing the salinity distribution in the mineralized zone are subject to modification. Such changes are made at each point representing the interface between adjacent ranges of *x*-values. Generally, at both sides of each such interfacial point, the salinity profile should be integrated over the mineralized zone. The results of such integrals represent the advected salinity flux at that point. Therefore, according to the mass conservation principle, both results of the integration should be identical, namely:

$$\left\{\int_0^{\delta_0} C dy\right\}_{left} = \left\{\int_0^{\delta_0} C dy\right\}_{right} \tag{A1}$$

where subscripts *left* and *right* refer to the upstream and downstream sides of the interfacial point, respectively. In relevant figures, like Figs. 6 and 11, these sides are represented as the left and right hand sides of the interfacial point, respectively.

In the following paragraphs the method of adjustment at each interfacial point is considered.

Downstream edge of the channel (curved channel)

The downstream edge of the channel, namely the point of $\xi = b/\sin\theta$, represents an interfacial point between the single BL developed on top of the channel, and the inner and outer BLs developed downstream of the channel edge. At this interfacial point, eq. (A1) yields:

$$\frac{1}{(n+1)}\{\delta_0 C_c\}_{left} = \left\{C_b \delta_u \left(\frac{n_1 + 0.5}{n_1 + 1}\right) + 0.5 C_b \left(\frac{\delta_0 - \delta_u}{n_2 + 1}\right)\right\}_{right} \tag{A2}$$

Equation (A2) incorporates 3 unknown quantities at the right hand side of channel edge, namely C_b, δ_u and δ_0. After some numerical experiments, we found it appropriate to keep the value of δ_0 unchanged, and to modify values of the other two parameters. We consider a hypothetical value of δ_u at the left-hand side of the channel edge, at which $C_a = 0.5C_c$, and assume that the salinity fluxes advected between the bottom of the aquifer and δ_u at both sides of the channel edge are identical. Therefore, the salinity fluxes advected between $y = \delta_u$ and $y = \delta_o$ are also identical at both sides of the channel edge. Introducing such an assumption into eq. (A2) we obtain:

$$\frac{(n_1+1)\left(1-0.5^{(n+1)/n}\right)}{(n+1)(n_1+0.5)}\{\delta_0 C_c\}_{left} = \{C_b\delta_u\}_{right} \tag{A3}$$

$$\frac{2\times 0.5^{(n+1)/n}(n_2+1)}{(n+1)}\{\delta_0 C_c\}_{left} = \{C_b(\delta_0-\delta_u)\}_{right} \tag{A4}$$

Equations (A3) and (A4) are applied to calculate values of C_b and δ_u at the right hand side of the channel edge. However, changes of values of obtained for C_b and δ_u are minor.

The attachment point

The attachment point represents the interface between the range of x-values at which the mineralized zone does not occupy the entire thickness of the aquifer, and the restructuring section, at which the entire thickness of the aquifer is mineralized. Employment of eq. (A1) for both sides of the attachment point yields:

$$\left\{C_b\delta_u\left[\frac{(n_1+0.5)}{(n_1+1)}\right]+C_b(B-\delta_u)\left(\frac{0.5}{n_2+1}\right)\right\}_{left} = \left\{C_b\delta_u\left[\frac{(n_3+0.5)}{(n_3+1)}\right]+C_b(B-\delta_u)\left(\frac{0.5}{n_4+1}\right)\right\}_{right} \tag{A5}$$

Equation (A5) incorporates 2 unknown quantities at the right hand side of the attachment point, namely C_b and, δ_u. Numerical experiments have indicated that salinity flux calculations could be useful to modify values of these two parameters. We assume that the salinity fluxes advected between the bottom of the aquifer and δ_u at both sides of the attachment point are identical. Therefore, the salinity fluxes advected between $y = \delta_u$ and $y = B$ are also identical at both sides of the channel edge. Introducing such an assumption into eq. (A5) we obtain:

$$\left\{C_b\delta_u\left[\frac{(n_1+0.5)}{(n_1+1)}\right]\right\}_{left} = \left\{C_b\delta_u\left[\frac{(n_3+0.5)}{(n_3+1)}\right]\right\}_{right} \tag{A6}$$

$$\left\{C_b(B-\delta_u)\frac{0.5}{n_2+1}\right\}_{left} = \left\{C_b(B-\delta_u)\frac{0.5}{n_4+1}\right\}_{right} \tag{A7}$$

Equations (A6) and (A7) are applied to calculate values of C_b and δ_u at the right hand side of the attachment point. However, changes of values obtained for C_b and δ_u are minor.

The establishment point

The establishment point represents the interface between the restructuring and establishment sections. Employment of eq. (A1) for both sides of the establishment point yields:

$$\left\{C_b\left[\left(\frac{n_3+0.5}{n_3+1}\right)+\left(\frac{0.5}{n_4+1}\right)\right]+C_t\left[\left(\frac{0.5}{n_3+1}\right)+\left(\frac{n_4+0.5}{n_4+1}\right)\right]\right\}_{left} = \left[C_b+C_t\right]_{right} \tag{A8}$$

Equation (A8) incorporates two unknown quantities, namely values of C_b and C_t at the right hand side of the establishment point. By assuming that identical salinity fluxes are conveyed through each one of the BLs at both sides of the establishment point, we obtain:

$$\left[C_b\left(\frac{n_3+0.5}{n_3+1}\right)+C_t\left(\frac{0.5}{n_3+1}\right)\right]_{left} = \left[C_b\left(\frac{n_5+0.5}{n_5+1}\right)+C_t\left(\frac{0.5}{n_5+1}\right)\right]_{right} \tag{A9}$$

$$\left[C_b\left(\frac{0.5}{n_4+1}\right)+C_t\left(\frac{n_4+0.5}{n_4+1}\right)\right]_{left} = \left[C_b\left(\frac{0.5}{n_4+1}\right)+C_t\left(\frac{n_4+0.5}{n_4+1}\right)\right]_{right} \tag{A10}$$

Equations (A9) and (A10) are used to calculate the values of C_b and C_t at the right hand side of the establishment point.

Upstream edge of the channel (winding channel) – mineralized zone smaller than aquifer thickness

In this case the left-hand side of the channel edge incorporates two BLs, which characterize the δ_0-development section. The right hand side of the channel edge is characterized by a single BL, as described by Fig. 6(b). Employment of eq. (A1) with regard to both sides of the channel edge yields:

$$\left\{C_b\delta_u\left[\frac{n_1(n_2+1)+c_r(n_2-n_1)}{(n_1+1)(n_2+1)}\right]+C_u\delta_0\frac{c_r}{n_2+1}\right\}_{left}=\left\{\left(\frac{1}{n+1}\right)C_c\delta_0\right\}_{right} \qquad \text{(A11)}$$

Equation (A11) is used to calculate the value of δ_0 at the right hand side of the channel edge.

Upstream edge of the channel (winding channel) – mineralized zone incorporates the entire aquifer thickness and is represented as a restructuring section

In this case the left-hand side of the channel edge incorporates two BLs, which characterize the restructuring section. The right hand side of the channel edge is characterized by a single BL, as described by Fig. 6(b), or 6(c). If the obtained value of δ_0 at the right hand side of the channel edge is smaller than the aquifer thickness then the employment of eq. (A1) with regard to both sides of the channel edge yields:

$$B\left\{C_t+(C_b-C_t)\frac{0.5}{n_4+1}+\frac{\delta_u}{B}(C_b-C_t)\left[\frac{n_3+0.5}{n_3+1}-\frac{0.5}{n_4+1}\right]\right\}_{left}=\left(\frac{C_c}{n+1}\right)\{\delta_0\}_{right} \qquad \text{(A12)}$$

Equation (A12) is used to calculate the value of δ_0 at the right hand side of the channel edge.

If eq.(A12) yields value of δ_0, which is larger than the aquifer thickness, then the right hand side of the channel edge is characterized by the salinity profile shown in Fig. 6(c). Under such conditions, the employment of eq. (A1) to both sides of the channel edge yields the following relationships:

$$\left\{C_t + (C_b - C_t)\frac{0.5}{n_4+1} + \frac{\delta_u}{B}(C_b - C_t)\left[\frac{n_3+0.5}{n_3+1} - \frac{0.5}{n_4+1}\right]\right\}_{left} = \left\{\frac{C_t n_6 + C_c}{n_6+1}\right\}_{right} \qquad \text{(A13)}$$

Equation (A13) is employed to calculate the value of C_t at the right hand side of the channel edge. This variable is the only unknown quantity in eq. (A13).

Upstream edge of the channel (winding channel) – mineralized zone incorporates the entire aquifer thickness and is represented as an establishment section

In this case the left-hand side of the channel edge incorporates two BLs, which characterize the establishment section. In such a section each BL incorporates half of the aquifer thickness. The right hand side of the channel edge is characterized by a single BL, as described by Fig. 6(b), or 6(c). If the obtained value of δ_0 at the right hand side of the channel edge is smaller than the aquifer thickness then the employment of eq. (A1) with regard to both sides of the channel edge yields:

$$\frac{B}{2}\{C_b + C_t\}_{left} = \left\{\left(\frac{1}{n+1}\right)C_c\delta_0\right\}_{right} \qquad \text{(A14)}$$

Equation (A14) is used to calculate the value of δ_0 at the right hand side of the channel edge.

If eq.(A14) yields value of δ_0, which is larger than the aquifer thickness, then the right hand side of the channel edge is characterized by the salinity profile shown in Fig. 6(c). Under such conditions, the application of eq. (A1) to both sides of the channel edge yields the following relationships:

$$\frac{1}{2}\{C_b + C_t\}_{left} = \left\{\frac{C_t n_6 + C_c}{n_6 + 1}\right\}_{right} \tag{A15}$$

Equation (A15) is employed to calculate the value of C_t at the right hand side of the channel edge. This variable is the only unknown quantity in eq. (A15).

Appendix B: Values of coefficients of eq. (26)

By the employment of BL approach and some assumptions with regards to mechanisms leading to the development of the inner BL in the restructuring section Rubin and Buddemeier (1998e) showed that the values of the coefficients β_i $(i = 1,\ldots 5)$ of eq. (26) are given by:

$$\beta_1 = \frac{2(n_1+0.5)\left(1-\frac{\delta_{u0}}{B}\right)\left(\frac{\delta_{u0}}{B}\right)\left[n_2(n_1+1)+n_1(n_2+0.5)\right]}{\left[2(n_1+0.5)(n_2+0.5)\left(\frac{\delta_{u0}}{B}\right)+(n_1+1)\left(1-\frac{\delta_{u0}}{B}\right)\right]^2} \tag{B1}$$

$$\beta_2 = \frac{2n_2(n_1+0.5)\left(\frac{\delta_{u0}}{B}\right)-n_1\left(1-\frac{\delta_{u0}}{B}\right)}{2\left[2(n_1+0.5)(n_2+0.5)\left(\frac{\delta_{u0}}{B}\right)+(n_1+1)\left(1-\frac{\delta_{u0}}{B}\right)\right]} \tag{B2}$$

$$\beta_3 = \frac{4(n_1+0.5)^2(n_2+0.5)\left(1-\frac{\delta_{u0}}{B}\right)\left(\frac{\delta_{u0}}{B}\right)^2\left[n_2(n_1+1)+n_1(n_2+0.5)\right]}{\left[2(n_1+0.5)(n_2+0.5)\left(\frac{\delta_{u0}}{B}\right)+(n_1+1)\left(1-\frac{\delta_{u0}}{B}\right)\right]^3} \tag{B3}$$

$$\beta_4 = 2(n_1+0.5)(n_2+0.5)\left(\frac{\delta_{u0}}{B}\right) \tag{B4}$$

$$\beta_5 = 2(n_1+0.5)(n_2+0.5)\left(\frac{\delta_{u0}}{B}\right)+(n_1+1)\left(1-\frac{\delta_{u0}}{B}\right) \tag{B5}$$

In eqs. (B1) – (B5), δ_{u0} is the thickness of the inner BL at the right hand side of the attachment point.

NOTATION

a	transverse dispersivity [L]
A_c	cross section area of the channel [L^2]
b	width of the channel [L]
B	thickness of the aquifer [L]
BL	boundary layer
cr	ratio between C_a and C_b at the boundary between the inner and outer BLs
C_a	salinity of the overlying aquifer [ML^{-3}]
C_{av}	average salinity of the overlying aquifer flowline [ML^{-3}]
C_c	salinity of the channel flow [ML^{-3}]
C_{c0}	salinity of reference of the channel flow, salinity at the channel entrance [ML^{-3}]
C_b	salinity at the bottom of the aquifer [ML^{-3}]
C_t	salinity at the top of the aquifer [ML^{-3}]
C_T	salinity at the top of the ROI, acceptable value of the salinity [ML^{-3}]
F	function defined in eq. (34)
J	number of channel segments comprising the dilution length
K_a	hydraulic conductivity of the aquifer [LT^{-1}]
K_c	hydraulic conductivity of the channel [LT^{-1}]
L_c	distance from the channel entrance to a cross section associated with the production of a particular value of C_{av}
L_D	dilution length of the channel [L]
L_E	establishment section length [L]
L_j	length of a channel segment [L]
L_R	restructuring section length [L]
m	number of the term in a series expansion

n, n_1, n_2, n_3, n_4, n_5, n_6 power coefficients of BL series expansions

q_a specific discharge of the aquifer flow [LT^{-1}]

Q_c flow-rate of the channel [L^3T^{-1}]

ROI region of interest

t time

T time interval measured from the initial contact between the saline channel water and the flowline of the overlying aquifer

TSBL top specified boundary layer

V_a flow velocity of the aquifer flow [LT^{-1}]

V_c flow velocity of the channel flow [LT^{-1}]

V_R the velocity ratio

x longitudinal coordinate [L]

x_{max} extent of the simulated domain [L]

x' coordinate extended along the channel centerline [L]

X longitudinal coordinate of the flowline extended downstream of the attachment point [L]

y transverse coordinate [L]

z vertical coordinate [L]

α_1 coefficient defined in eq. (15)

α_2 coefficient defined in eq. (16)

α_3 coefficient defined in eq. (31)

β_i $(i=1,..5)$ coefficient defined in Appendix B

γ coefficient defined in eq. (26)

δ thickness of the ROI [L]

δ_u thickness of the inner BL [L]

δ_{u0} thickness of the inner BL at the right hand side of the attachment point [L]

δ_0 thickness of the mineralized zone [L]

Δx longitudinal interval [L]

ζ outer BL coordinate

ζ_T value of ζ at the top of the ROI

η BL coordinate

η_T value of η at the top of the ROI

θ angle of orientation of the channel

λ inner BL coordinate

λ_T value of λ at the top of the ROI

ξ local coordinate of the interface of direct contact [L]

ϕ_a porosity of the aquifer

ϕ_c porosity of the channel

ω BL coordinate used at the direct contact interface where the mineralized zone occupies the entire thickness of the aquifer

REFERENCES

Buddemeier, R.W., Sophocleous, M.A. and Whittemore, D.O., 1992. Mineral intrusion—Investigation of salt contamination of groundwater in the Eastern Great Bend Prairie Aquifer, Open-File Rept. 92-25, Geohydrology, Kansas Geological Survey, The University of Kansas, Lawrence, KS.

Buddemeier, R.W., Garneau, G.W., Young, D.P., Whittemore, D.O., Zehr, D., Lanterman, J., Ma, T.S., and Falk, S., 1994. The mineral intrusion project: Progress and activities during fiscal year 1994, Open-File Rept. 94-28, Geohydrology, Kansas Geological Survey, The University of Kansas, Lawrence, KS.

Caralaw, H.S. and Jaeger, J.C., 1959. "Conduction of Heat in Solids", p. 100, 2nd edition, Clarendon Press, Oxford, England

Cobb, P.M., 1980. The distribution and mechanisms of salt water intrusion in the fresh water aquifer and in Rattlesnake Creek Stafford County Kansas, M.S. thesis, Department of Civil Engineering, The University of Kansas, Lawrence, KS.

Fader, S.W. and Stullken, L.E., 1978. Geohydrology of the Great Bend Prairie South-Central Kansas, Irrigation Series 4, Kansas Geological Survey.

Fischer, H.B., List, E., Koh, R.C.Y., Imberger, J. and Brooks, N.H., 1979. Mixing in Inland and Coastal Waters, Academic Press, NY.

Garneau, G.W., 1995. Detection and characterization of the distribution of mineral intrusion in the Great Bend Prairie aquifer - south-central Kansas, Open-file Report 95-35, Kansas Geological Survey, The University of Kansas, Lawrence, Kansas.

Latta, B., 1950. Geology and groundwater resources of Barton and Stafford Counties, Kansas Bulletin 88, Kansas Geological Survey.

Layton, D.W. and Berry, D.W., 1973. Geology and ground-water resources of Pratt County, South-Central Kansas, Bulletin 205, Kansas Geological Survey.

Rubin, H. and Atkinson, J.F., 1998. Boundary layer analysis of contaminant mixing in a river, paper under review.

Rubin, H. and Buddemeier, R.W., 1996. A top specified boundary layer (TSBL) approximation approach for the simulation of groundwater contamination processes, Journal of Contaminant Hydrology, 22: 123 – 144.

Rubin, H. and Buddemeier, R.W., 1998a. Application of the top specified boundary layer (TSBL) approximation to initial characterization of an inland aquifer mineralization, Part 1: Direct contact between fresh and saltwarer, Journal of Contaminant Hydrology, 32/3-4: 149-172.

Rubin, H. and Buddemeier, R.W., 1998b. Application of the top specified boundary layer (TSBL) approximation to initial characterization of an inland aquifer mineralization, Part 2: Seepage of saltwater through semi-confining layers, Journal of Contaminant Hydrology, 32/3-4: 173-198.

Rubin, H. and Buddemeier, R.W., 1998c. Approximate analysis of groundwater mineralization due to local discontinuities in impermeable layer - Part 1 Direct contact between fresh and saltwater, Open-File Rept. 98-31, Kansas Geological Survey, the University of Kansas, Lawrence, Kansas.

Rubin, H., and Buddemeier, R.W., 1998d. Approximate analysis of groundwater mineralization due to local discontinuities in impermeable layer - Part 2: Seepage of saltwater through semi-confining discontinuity, Open-File Rept. 98-32, Kansas Geological Survey, the University of Kansas, Lawrence, Kansas.

Rubin, H., and Buddemeier, R.W., 1998e. Approximate analysis of aquifer mineralization due to horizontal penetration of salinity, Open-File Rept. 98-33, Kansas Geological Survey, the University of Kansas, Lawrence, Kansas.

Sophocleous, M.A., 1991. Stream-floodwater propagation through the Great Bend alluvial aquifer Kansas - Field measurements and numerical simulations, Journal of Hydrology, 124: 207-228.

Whittemore, D.O., 1993. Ground water geochemistry in the mineral intrusion area of groundwater management district no. 5, South-Central Kansas, Kansas Geological Survey, The University of Kansas, Lawrence, Kansas.

Young, D.P., 1992. Mineral intrusion: Geohydrology of Permian bedrock underlying the Great Bend Prairie aquifer in south-central Kansas, Open-File Rept. 92-44, Geohydrology, Kansas

Geological Survey, The University of Kansas, Lawrence, Kansas.

Young, D. and Rubin, H., 1998. Determining vertical flow in variable density groundwater - a hydrostatic approach applied in south-central Kansas, Eighteenth Annual Hydrology Days, Colorado State University, Fort Collins, Colorado, March 30-April 3, 1998